Pyridine-based 1,2,4-triazolo tethered indole conjugates potentially affecting TNKS and PI3K in colorectal cancer

Prasanna A. Yakkala,[¶,‡] Samir R. Panda, [†,‡] Vegi G.M. Naidu,[†*] Syed Shafi[#*] and Ahmed Kamal[¶,ǁ*]

[¶]*Department of Pharmaceutical Chemistry, School of Pharmaceutical Education and Research, Jamia Hamdard, New Delhi 110062, India*

[†]*Department of Pharmacology and Toxicology, National Institute of Pharmaceutical Education and Research (NIPER)-Guwahati, Assam 781101, India*

[#]*Department of Chemistry, School of Chemical and Life Sciences, Jamia Hamdard, New Delhi, India*

[ǁ]*Department of Pharmacy, Birla Institute of Technology & Science, Pilani; Hyderabad Campus, Hyderabad 500078, TS, India*

‡ These authors contributed equally to this work

*Correspondence E-mail: ahmedkamal@iict.res.in; ahmedkamal@hyderabad.bits-pilani.ac.in; syedshafi@jamiahamdard.ac.in; vgmnaidu@niperguwahati.ac.in

List of the Contents

General procedure for synthesis and biological evaluation of (14a-q)…….…….. S2–S30

MD trajectory analysis…….……..…..... S31–S34

Reference ……..…..... S35–S38

^{1}H NMR and ^{13}C NMR copies of all products …….……....S39–S57

HPLC data…….…..…….. S58–S59

Materials and methods

Compound library selection

Literature studies and various databases have discovered that 1,2,4-triazoles containing molecules and their derivatives have shown effective activity against HT-29, CACO2 and DLD1 colon cell lines for screening of anti-cancer properties [1]. Therefore, the substructure search was carried out in ZINC 15 and PubChem database using 1,2,4-triazoles and pyridine based 1,2,4-triazoles as the query molecules, all the 150 hits generated were included as one set of libraries for the virtual screening [2]. Further, pyridine containing 1,2,4-triazoles have been reported to inhibit the tankyrase proteins. Thus, pyridine based 1,2,4-triazolo tethered with the indole moiety was used as a second query molecule in the ZINC 15 database and all the hits were generated. Later, the set of these molecules was docked and passed through the PAINS filter.

Table S1. Designed molecules and docking scores

S. No	Smiles	Xp G score (kcal/mol) 3L54	Xp G score (kcal/mol) 4OA7
1	CC1=CC=CC=C1N2C(SCC(C3=CNC4=C3C=CC=C4)=O)=NN=C2C5=CC=NC=C5	-3.141	-5.781
2	O=C(C1=CNC2=C1C=CC=C2)C(C3=CC=CC=C3)SC4=NN=C(C5=CC=NC=C5)N4C6=CC=CC=C6	-2.221	-3.508
3	CCN1C=C(C(CSC2=NN=C(C3=CC=NC=C3)N2C4=CC=C(C)C(C)=C4)=O)C5=C1C=CC=C5	-3.482	-5.463
4	CC(SC1=NN=C(C2=CC=NC=C2)N1C3=CC=CC=C3)C(C4=CNC5=C4C=CC=C5)=O	-5.125	-7.385
5	CCC1=CC=CC2=C1NC=C2C(CSC3=NN=C(C4=CC=NC=C4)N3C5=CC=CC=C5)=O	-5.039	-7.896
6	CN1C=C(C(CSC2=NN=C(C3=CC=NC=C3)N2C4=CC=CC=C4)=O)C5=C1C=CC=C5	-4.566	-7.554

7	CCN1C=C(C(CSC2=NN=C(C3=CC=NC=C3)N2C4=CC=CC=C4)=O)C5=C1C=CC=C5	-4.117	-7.321
8	O=C(C1=CNC2=C1C=CC=C2)[C@H](C3=CC=CC=C3)SC4=NN=C(C5=CC=NC=C5)N4C6=CC=CC=C6	-3.477	-3.220
9	O=C(C1=CNC2=C1C=CC=C2)[C@@H](C3=CC=CC=C3)SC4=NN=C(C5=CC=NC=C5)N4C6=CC=CC=C6	-3.142	-3.451
10	CCC1=CC=C(N2C(S[C@H](C3=CC=CC=C3)C(C4=CNC5=C4C=CC=C5)=O)=NN=C2C6=CC=NC=C6)C=C1	-2.895	-2.171
11	CCC1=CC=C(N2C(S[C@@H](C3=CC=CC=C3)C(C4=CNC5=C4C=CC=C5)=O)=NN=C2C6=CC=NC=C6)C=C1	-2.771	-2.896
12	CC1=CC=C(N2C(SCC(C3=CNC4=C3C=CC=C4)=O)=NN=C2C5=CC=NC=C5)C=C1C	-3.687	-6.935
13	CC(N1)=C(C(CSC2=NN=C(C3=CC=NC=C3)N2C4=CC=C(C)C(C)=C4)=O)C5=C1C=CC=C5	-3.110	-6.253
14	CC(N1)=C(C(CSC2=NN=C(C3=CC=NC=C3)N2C4=CC=CC=C4)=O)C5=C1C=CC=C5	-4.101	-7.557
15	N#CCCN1C=C(C(CSC2=NN=C(C3=CC=NC=C3)N2C4=CC=C(C)C(C)=C4)=O)C5=C1C=CC=C5	-2.302	-6.129
16	N#CCCN1C=C(C(CSC2=NN=C(C3=CC=NC=C3)N2C4=CC=CC=C4C)=O)C5=C1C=CC=C5	-2.864	-6.827
17	N#CCCN1C=C(C(CSC2=NN=C(C3=CC=NC=C3)N2C4=CC=C(Cl)C=C4)=O)C5=C1C=CC=C5	-5.571	-6.204

18	CC(N1)=C(C(CSC2=NN=C(C3=CC=NC=C3)N2C4=CC=C(Cl)C=C4)=O)C5=C1C=CC=C5	-4.919	-7.331
19	N#CCCN1C=C(C(CSC2=NN=C(C3=CC=NC=C3)N2C4=CC=CC=C4)=O)C5=C1C=CC=C5	-5.673	-7.765
20	FC(F)(F)CN1C(SCC(C2=C(C)NC3=C2C=CC=C3)=O)=NN=C1C4=CC=NC=C4	-4.449	-9.409
21	CC(SC1=NN=C(C2=CC=NC=C2)N1CC(F)(F)F)C(C3=C(C)NC4=C3C=CC=C4)=O	-5.504	-9.469
22	CC(SC1=NN=C(C2=CC=NC=C2)N1C3=CC=C(F)C=C3)C(C4=C(C)NC5=C4C=CC=C5)=O	-5.231	-8.008
23	FC1=CC=C(N2C(SCC(C3=CNC4=C3C=CC=C4CC)=O)=NN=C2C5=CC=NC=C5)C=C1	-4.888	-6.821
24	FC1=CC=C(N2C(SCC(C3=CNC4=C3C=CC=C4)=O)=NN=C2C5=CC=NC=C5)C=C1	-5.686	-8.134
25	O=C(C1=CNC2=C1C=CC=C2)CSC3=NN=C(C4=CC=NC=C4)N3CC5=CC=CO5	-5.185	-9.148
26	O=C(C1=C(C)NC2=C1C=CC=C2)CSC3=NN=C(C4=CC=NC=C4)N3CC=C	-4.761	-6.889
27	O=C(C1=CNC2=C1C=CC=C2CC)CSC3=NN=C(C4=CC=NC=C4)N3C	-3.226	-5.153
28	O=C(C1=CNC2=C1C=CC=C2)CSC3=NN=C(C4=CC=NC=C4)N3CCOC	-5.115	-9.330
29	O=C(C1=C(C2=CC=CC=C2)N(C)C3=C1C=CC=C3)CSC4=NN=C(C5=CC=NC=C5)N4CCOC	-3.625	-5.65
30	O=C(C1=C(C)NC2=C1C=CC=C2)CSC3=NN=C(C4=CC=NC=C4)N3C	-4.863	-8.484
31	O=C(C1=CNC2=C1C=CC=C2)CSC3=NN=C(C4=CC=NC=C4)N3CC5=CC=CC=C5	-4.673	-7.889

32	C=CCN1C(SC(C2=CC=CC=C2)C(C3=CNC4=C3C=CC=C4)=O)=NN=C1C5=CC=NC=C5	-3.920	-8.214
33	C=CCN1C(SCC(C2=CNC3=C2C=CC=C3CC)=O)=NN=C1C4=CC=NC=C4	-5.741	-7.235
34	CCCN1C(SCC(C2=CNC3=C2C=CC=C3CC)=O)=NN=C1C4=CC=NC=C4	-5.829	-8.883
35	CCN1C(SCC(C2=CNC3=C2C=CC=C3)=O)=NN=C1C4=CC=NC=C4	-3.268	-6.779
36	CCN1C(SCC(C2=CNC3=C2C=CC=C3CC)=O)=NN=C1C4=CC=NC=C4	-3.251	-8.921
37	C[C@H](SC1=NN=C(C2=CC=NC=C2)N1CCC)C(C3=CNC4=C3C=CC=C4)=O	-4.236	-9.084
38	CCN1C(SCC(C2=C(C)N(CC)C3=C2C=CC=C3)=O)=NN=C1C4=CC=NC=C4	-4.788	-8.907
39	O=C(C1=C(C)NC2=C1C=CC=C2)CSC3=NN=C(C4=CC=NC=C4)N3C5CC5	-3.856	-5.864
40	CCC1=CC=CC2=C1NC=C2C(CSC3=NN=C(C4=CC=NC=C4)N3C5CC5)=O	-3.259	-6.216
41	COCCN1C(SCC(C2=CNC3=C2C=CC=C3CC)=O)=NN=C1C4=CC=NC=C4	-5.584	-8.625
42	O=C(C1=C(C2=CC=CC=C2)NC3=C1C=CC=C3)CSC4=NN=C(C5=CC=NC=C5)N4CC	-3.315	-6.986
43	CC(SC1=NN=C(C2=CC=NC=C2)N1C3CC3)C(C4=C(C)NC5=C4C=CC=C5)=O	-3.747	-8.596
44	N#CCCN1C=C(C(CSC2=NN=C(C3=CC=NC=C3)N2C4CC4)=O)C5=C1C=CC=C5	-2.951	-6.775
45	CN1C(SC(C2=CC=CC=C2)C(C3=CNC4=C3C=CC=C4CC)=O)=NN=C1C5=CC=NC=C5	-3.338	-3.158
46	CC(C)CN1C(SCC(C2=CN(C)C3=C2C=CC=C3)=O)=NN=C1C4=CC=NC=C4	-4.167	-2.849

47	C[C@H](SC1=NN=C(C2=CC=NC=C2)N1CCCOCC)C(C3=C(C)NC4=C3C=CC=C4)=O	-5.273	-9.032
48	CCCN1C(SCC(C2=C(C3=CC=CC=C3)NC4=C2C=CC=C4)=O)=NN=C1C5=CC=NC=C5	-4.867	-3.981
49	CC(SC1=NN=C(C2=CC=NC=C2)N1CCC)C(C3=C(C)NC4=C3C=CC=C4)=O	-5.745	-8.488
50	COCCN1C(SC(C2=CC=CC=C2)C(C3=CNC4=C3C=CC=C4CC)=O)=NN=C1C5=CC=NC=C5	-3.916	-5.032
51	N#CCCN1C=C(C(CSC2=NN=C(C3=CC=NC=C3)N2CCC)=O)C4=C1C=CC=C4	-4.759	-8.071
52	N#CCCN1C=C(C(CSC2=NN=C(C3=CC=NC=C3)N2CCOC)=O)C4=C1C=CC=C4	-4.071	-9.408
53	ClC1=CC=CC(N2C(SCCC3=CNC4=CC=CC=C43)=NN=C2C5=CC=NC=C5)=C1	-3.714	-6.540
54	ClC(C=C1)=CC=C1N2C(SCCC3=CNC4=CC=CC=C43)=NN=C2C5=CC=NC=C5	-5.918	-7.033
55	CN1C(C2=CC=NC=C2)=NN=C1SCCC3=CNC4=C3C=CC=C4	-5.399	-9.817
56	CCN1C(C2=CC=NC=C2)=NN=C1SCCC3=CNC4=C3C=CC=C4	-4.684	-8.081
57	CCCN1C(C2=CC=NC=C2)=NN=C1SCCC3=CNC4=C3C=CC=C4	-3.715	-8.597
58	CCCCN1C(C2=CC=NC=C2)=NN=C1SCCC3=CNC4=C3C=CC=C4	-5.065	-8.889
59	CCCCCN1C(C2=CC=NC=C2)=NN=C1SCCC3=CNC4=C3C=CC=C4	-3.223	-8.412
60	CC(C)CCN1C(C2=CC=NC=C2)=NN=C1SCCC3=CNC4=C3C=CC=C4	-3.716	-8.932

61	CC(C)N1C(C2=CC=NC=C2)=NN=C1SCCC3=CNC4=C3C=CC=C4	-3.382	-8.906
62	C1(C2=NN=C(SCCC3=CNC4=C3C=CC=C4)N2C5CC5)=CC=NC=C1	-4.351	-8.557
63	C1(C2=NN=C(SCCC3=CNC4=C3C=CC=C4)N2C5CCC5)=CC=NC=C1	-4.199	-8.923
64	C1(C2=NN=C(SCCC3=CNC4=C3C=CC=C4)N2C5CCCC5)=CC=NC=C1	-5.481	-7.515
65	C1(C2=NN=C(SCCC3=CNC4=C3C=CC=C4)N2C5CCCCC5)=CC=NC=C1	-3.596	-8.624
66	C1(C2=NN=C(SCCC3=CNC4=C3C=CC=C4)N2C5CCCCCC5)=CC=NC=C1	-4.373	-7.873
67	C1(C2=NN=C(SCCC3=CNC4=C3C=CC=C4)N2C5CCCCCCC5)=CC=NC=C1	-4.600	-7.609
68	C=CCN1C(C2=CC=NC=C2)=NN=C1SCCC3=CNC4=C3C=CC=C4	-5.04	-8.888
69	C1(C2=NN=C(SCCC3=CNC4=C3C=CC=C4)N2C5=CC=CN5)=CC=NC=C1	-4.205	-7.685
70	C1(C2=NN=C(SCCC3=CNC4=C3C=CC=C4)N2C5=CC=CO5)=CC=NC=C1	-3.448	-7.810
71	C1(C2=NN=C(SCCC3=CNC4=C3C=CC=C4)N2C5=CC=CS5)=CC=NC=C1	-3.179	-6.996
72	C1(C2=NN=C(SCCC3=CNC4=C3C=CC=C4)N2C5=CN=CN5)=CC=NC=C1	-2.127	-5.152
73	C1(C2=NN=C(SCCC3=CNC4=C3C=CC=C4)N2C5=CN=CO5)=CC=NC=C1	-2.896	-4.858
74	C1(C2=NN=C(SCCC3=CNC4=C3C=CC=C4)N2C5=CN=CS5)=CC=NC=C1	-2.997	-5.967
75	C1(C2=NN=C(SCCC3=CNC4=C3C=CC=C4)N2C5=NC=CN5)=CC=NC=C1	-3.111	-4.96

76	C1(C2=NN=C(SC3=CNC4=C3C=CC=C4)N2CC5=CC=CC=C5)=CC=NC=C1	-4.999	-7.735
77	C1(C2=NN=C(SCC3=CNC4=C3C=CC=C4)N2CC5=CC=CC=C5)=CC=NC=C1	-5.288	-8.612
78	C1(C2=NN=C(SCCC3=CNC4=C3C=CC=C4)N2CC5=CC=CC=C5)=CC=NC=C1	-5.674	-8.887
79	C1(C2=NN=C(SCCCC3=CNC4=C3C=CC=C4)N2CC5=CC=CC=C5)=CC=NC=C1	-3.825	-8.014
80	C1(C2=NN=C(SCCC3=CNC4=C3C=CC=C4)N2C5=CC=CC=C5)=CC=NC=C1	-3.651	-9.105
81	C1(C2=NN=C(SCCC3=CNC4=C3C=CC=C4)N2C5=CC=NC=C5)=CC=NC=C1	-3.879	-7.456
82	C1(C2=NN=C(SCCC3=CNC4=C3C=CC=C4)N2C5=CC=CN=C5)=CC=NC=C1	-3.232	-7.158
83	C1(C2=NN=C(SCCC3=CNC4=C3C=CC=C4)N2C5=CC=CC=N5)=CC=NC=C1	-4.175	-7.756
84	CC1=CC=CC=C1N2C(C3=CC=NC=C3)=NN=C2SCCC4=CNC5=C4C=CC=C5	-5.487	-6.457
85	CC1=CC(N2C(C3=CC=NC=C3)=NN=C2SCCC4=CNC5=C4C=CC=C5)=CC=C1	-5.281	-7.551
86	CC(C=C1)=CC=C1N2C(C3=CC=NC=C3)=NN=C2SCCC4=CNC5=C4C=CC=C5	-3.732	-8.097
87	FC1=CC=CC=C1N2C(C3=CC=NC=C3)=NN=C2SCCC4=CNC5=C4C=CC=C5	-6.052	-9.747
88	FC1=CC(N2C(C3=CC=NC=C3)=NN=C2SCCC4=CNC5=C4C=CC=C5)=CC=C1	-5.564	-8.852
89	FC(C=C1)=CC=C1N2C(C3=CC=NC=C3)=NN=C2SCCC4=CNC5=C4C=CC=C5	-5.376	-8.934
90	BrC1=CC=CC=C1N2C(C3=CC=NC=C3)=NN=C2SCCC4=CNC5=C4C=CC=C5	-4.103	-5.780

91	BrC1=CC(N2C(C3=CC=NC=C3)=NN=C2SCCC4=CNC5=C4C=CC=C5)=CC=C1	-5.038	-7.376
92	BrC(C=C1)=CC=C1N2C(C3=CC=NC=C3)=NN=C2SCCC4=CNC5=C4C=CC=C5	-4.352	-6.389
93	CC1=CC(N2C(C3=CC=NC=C3)=NN=C2SCCC4=CNC5=C4C=CC=C5)=CC(C)=C1	-6.037	-7.476
94	CC1=CC(N2C(C3=CC=NC=C3)=NN=C2SCCC4=CNC5=C4C=CC=C5)=CC(C)=C1	-5.348	-5.871
95	FC1=CC=CC(F)=C1N2C(C3=CC=NC=C3)=NN=C2SCCC4=CNC5=C4C=CC=C5	-5.593	-7.885
96	FC1=CC(N2C(C3=CC=NC=C3)=NN=C2SCCC4=CNC5=C4C=CC=C5)=CC(F)=C1	-4.988	-6.565
97	ClC1=CC=CC(Cl)=C1N2C(C3=CC=NC=C3)=NN=C2SCCC4=CNC5=C4C=CC=C5	-4.751	-5.198
98	ClC1=CC(N2C(C3=CC=NC=C3)=NN=C2SCCC4=CNC5=C4C=CC=C5)=CC(Cl)=C1	-3.986	-5.583
99	BrC1=CC=CC(Br)=C1N2C(C3=CC=NC=C3)=NN=C2SCCC4=CNC5=C4C=CC=C5	-5.247	-6.932
100	BrC1=CC(N2C(C3=CC=NC=C3)=NN=C2SCCC4=CNC5=C4C=CC=C5)=CC(Br)=C1	-4.259	-6.228
101	OC1=CC=CC=C1N2C(C3=CC=NC=C3)=NN=C2SCCC4=CNC5=C4C=CC=C5	-3.322	-5.147
102	OC1=CC(N2C(C3=CC=NC=C3)=NN=C2SCCC4=CNC5=C4C=CC=C5)=CC=C1	-2.961	-6.007
103	OC(C=C1)=CC=C1N2C(C3=CC=NC=C3)=NN=C2SCCC4=CNC5=C4C=CC=C5	-2.568	-5.746
104	NC1=CC=CC=C1N2C(C3=CC=NC=C3)=NN=C2SCCC4=CNC5=C4C=CC=C5	-3.886	-5.401
105	NC1=CC(N2C(C3=CC=NC=C3)=NN=C2SCCC4=CNC5=C4C=CC=C5)=CC=C1	-4.004	-6.052

106	NC(C=C1)=CC=C1N2C(C3=CC=NC=C3)=NN=C2SCCC4=CNC5=C4C=CC=C5	-3.51	-5.996
107	O=[N+](C1=CC=CC=C1N2C(C3=CC=NC=C3)=NN=C2SCCC4=CNC5=C4C=CC=C5)[O-]	-5.341	-7.426
108	O=[N+](C1=CC(N2C(C3=CC=NC=C3)=NN=C2SCCC4=CNC5=C4C=CC=C5)=CC=C1)[O-]	-5.147	-7.101
109	O=[N+](C(C=C1)=CC=C1N2C(C3=CC=NC=C3)=NN=C2SCCC4=CNC5=C4C=CC=C5)[O-]	-5.347	-8.010
110	O=[N+](C1=CC=CC([N+]([O-])=O)=C1N2C(C3=CC=NC=C3)=NN=C2SCCC4=CNC5=C4C=CC=C5)[O-]	-4.685	-6.231
111	O=[N+](C1=CC(N2C(C3=CC=NC=C3)=NN=C2SCCC4=CNC5=C4C=CC=C5)=CC([N+]([O-])=O)=C1)[O-]	-4.153	-5.897
112	NC1=CC=CC(N)=C1N2C(C3=CC=NC=C3)=NN=C2SCCC4=CNC5=C4C=CC=C5	-4.174	-3.221
113	NC1=CC(N2C(C3=CC=NC=C3)=NN=C2SCCC4=CNC5=C4C=CC=C5)=CC(N)=C1	-4.925	-3.562
114	OC1=CC=CC(O)=C1N2C(C3=CC=NC=C3)=NN=C2SCCC4=CNC5=C4C=CC=C5	-3.189	-6.845
115	OC1=CC(N2C(C3=CC=NC=C3)=NN=C2SCCC4=CNC5=C4C=CC=C5)=CC(O)=C1	-3.339	-7.152
116	COC1=CC=CC=C1N2C(C3=CC=NC=C3)=NN=C2SCCC4=CNC5=C4C=CC=C5	-5.155	-7.188
117	COC1=CC(N2C(C3=CC=NC=C3)=NN=C2SCCC4=CNC5=C4C=CC=C5)=CC=C1	-5.971	-7.034
118	COC(C=C1)=CC=C1N2C(C3=CC=NC=C3)=NN=C2SCCC4=CNC5=C4C=CC=C5	-6.590	-9.748

119	COC1=CC=CC(OC)=C1N2C(C3=CC=NC=C3)=NN=C2SCCC4=CNC5=C4C=CC=C5	-5.201	-6.256
120	COC1=CC(N2C(C3=CC=NC=C3)=NN=C2SCCC4=CNC5=C4C=CC=C5)=CC(OC)=C1	-5.578	-7.109
121	COC(C(OC)=C1)=C(OC)C=C1N2C(C3=CC=NC=C3)=NN=C2SCCC4=CNC5=C4C=CC=C5	-6.226	-9.247
122	CCOC1=CC=CC(OCC)=C1N2C(C3=CC=NC=C3)=NN=C2SCCC4=CNC5=C4C=CC=C5	-3.479	-7.421
123	CCOC1=CC(N2C(C3=CC=NC=C3)=NN=C2SCCC4=CNC5=C4C=CC=C5)=CC(OCC)=C1	-2.856	-7.051
124	CCOC1=C(OCC)C(OCC)=CC(N2C(C3=CC=NC=C3)=NN=C2SCCC4=CNC5=C4C=CC=C5)=C1	-3.519	-8.224
125	CCOC1=CC=CC=C1N2C(C3=CC=NC=C3)=NN=C2SCCC4=CNC5=C4C=CC=C5	-2.753	-5.876
126	CCOC1=CC(N2C(C3=CC=NC=C3)=NN=C2SCCC4=CNC5=C4C=CC=C5)=CC=C1	-2.159	-6.215
127	CCOC(C=C1)=CC=C1N2C(C3=CC=NC=C3)=NN=C2SCCC4=CNC5=C4C=CC=C5	-3.997	-5.880
128	COC(C=C1)=CC=C1N2C(SCC3=CNC4=CC=CC=C43)=NN=C2C5=CC=NC=C5	-4.989	-8.101
129	COC(C=C1)=CC=C1N2C(SCCCC3=CNC4=CC=CC=C43)=NN=C2C5=CC=NC=C5	-4.382	-7.486
130	CCCCN1C(SCC2=CNC3=CC=CC=C32)=NN=C1C4=CC=NC=C4	-5.023	-7.775
131	CCCCN1C(SCCCC2=CNC3=CC=CC=C32)=NN=C1C4=CC=NC=C4	-5.088	-6.898
132	C=CCN1C(SCC2=CNC3=CC=CC=C32)=NN=C1C4=CC=NC=C4	-4.821	-7.123

133	C=CCN1C(SCCCC2=CNC3=CC=CC=C32)=NN=C1C4=CC=NC=C4	-3.712	-6.862
134	O=C(NC1=CC2=C(C=C1)N(CC)C3=C2C=CC=C3)CSC4=NN=C(C5=CC=NC=C5)N4CC	-2.865	-6.374
135	FC1=CC2=C(C=C1)C(CC3=NN=C(SC4=CC=CN=C4)N3CCCC5=CCC=N5)=CN2	-4.905	-6.373
136	O=C(N[C@H](C1=NN=C(SCC2=CC=NC=C2)N1C3=CC=C(OC)C=C3)CC4=CC=CC=C4)CC5=C(C)NC6=C5C=CC=C6	-2.117	-4.568
137	O=C(N[C@H](C1=NN=C(SCC2=CC=CN=C2)N1C3=CC=C(OC)C=C3)CC4=CC=CC=C4)CC5=C(C)NC6=C5C=CC=C6	-2.329	-3.117
138	O=C(N[C@H](C1=NN=C(SCC2=NC=CC=C2)N1C3=CC=C(OC)C=C3)CC4=CC=CC=C4)CC5=C(C)NC6=C5C=CC=C6	-2.881	-3.143
139	CC(N1)=C(C(CSC2=NN=C(C3=CC=NC=C3)N2C4=CC=C(OC)C=C4)=O)C5=C1C=CC=C5	-5.011	-6.593
140	COC1=CC=C(N2C(SCC(C3=CNC4=C3C=CC=C4CC)=O)=NN=C2C5=CC=NC=C5)C=C1	-5.516	-7.122
141	COC1=CC=C(N2C(SCC(C3=CNC4=C3C=CC=C4)=O)=NN=C2C5=CC=NC=C5)C=C1	-5.938	-7.559
142	CC(SC1=NN=C(C2=CC=NC=C2)N1C3=CC=C(OC)C=C3)C(C4=C(C)NC5=C4C=CC=C5)=O	-5.124	-7.312
143	COC1=CC=C(N2C(SCC(C3=CN(CC)C4=C3C=CC=C4)=O)=NN=C2C5=CC=NC=C5)C=C1	-6.001	-5.060
144	CC(SC1=NN=C(C2=CC=NC=C2)N1C3=CC=C(OCC)C=C3)C(C4=CNC5=C4C=CC=C5)=O	-3.258	-6.159

145	CC(N1)=C(C(CSC2=NN=C(C3=CC=NC=C3)N2C4=CC=C(OCC)C=C4)=O)C5=C1C=CC=C5	-3.030	-5.999
146	CC(SC1=NN=C(C2=CC=NC=C2)N1C3=CC=C(OC)C=C3)C(C4=CNC5=C4C=CC=C5)=O	-4.65	-7.789
147	O=C(C1=CNC2=C1C=CC=C2)CSC3=NN=C(C4=CC=NC=C4)N3C5=CC=CC=C5	-5.156	-7.880
148	O=C(C1=CNC2=C1C=CC=C2)CSC3=NN=C(C4=CC=NC=C4)N3C5=CC=CC(Cl)=C5C	-4.873	-6.568
149	CN1C(C2=CC=CC=C2)=C(C(CSC3=NN=C(C4=CC=NC=C4)N3C5=CC=CC(Cl)=C5C)=O)C6=C1C=CC=C6	-5.085	-8.383
150	CCC1=CC=C(N2C(SCC(C3=CNC4=C3C=CC=C4)=O)=NN=C2C5=CC=NC=C5)C=C1	-4.785	-3.545
151	CCC1=CC=C(N2C(SC(C3=CC=CC=C3)C(C4=CNC5=C4C=CC=C5)=O)=NN=C2C6=CC=NC=C6)C=C1	-4.137	-3.248
152	O=C(C1=C(C)NC2=C1C=CC=C2)CSC3=NN=C(C4=CC=NC=C4)N3C5=CC=C(Cl)C(Cl)=C5	-5.491	-7.159
153	CCC1=CC=CC2=C1NC=C2C(CSC3=NN=C(C4=CC=NC=C4)N3C5=CC=C(Cl)C(Cl)=C5)=O	-4.861	-6.244
154	CC1=CC=CC=C1N2C(SCC(C3=C(C)NC4=C3C=CC=C4)=O)=NN=C2C5=CC=NC=C5	-4.601	-5.103
155	O=C(NC1=CC2=C(C=C1)N(CC)C3=C2C=CC=C3)CSC4=NN=C(C5=CC=NC=C5)N4C6=CC=C(OC)C=C6	-2.113	-5.861

156	O=C(NC1=CC=C(C=CC=C2)C2=C1)CSC3=NN=C(C4=CC=NC=C4)N3C5=CC=C(OC)C=C5	-1.981	-4.806
157	O=C(NC1=CC(C(C=CC=C2)C2C1=O)=O)CSC3=NN=C(C4=CC=NC=C4)N3C5=CC=C(OC)C=C5	-3.212	-6.175
158	COC(C=C1)=CC=C1N2C(SCC3=NN=NC3C4=CC=C(OC)C=C4)=NN=C2C5=CC=NC=C5	-4.176	-7.283
159	O=C(N1C=NC2=NC=NC=C12)CSC3=NN=C(C4=CC=NC=C4)N3C5=CC=C(OC)C=C5	-5.118	-4.217
160	O=C(NC1CCC(OC2=CC=C(C#N)C=C2)CC1)CSC3=NN=C(C4=CC=NC=C4)N3C5=CC=C(OC)C=C5	-2.818	-9.750
161	O=C(NC1=C(C)N(C)N(C2=CC=CC=C2)C1=O)CSC3=NN=C(C4=CC=NC=C4)N3C5=CC=C(OC)C=C5	-3.855	-6.781

Molecular modeling

The virtually designed molecules were *in-silico* evaluated by molecular docking and were docked with the protein (PDB ID: 4OA7 & 3L54) for tankyrase and PI3K respectively. Molecular docking of virtually synthesized molecules was performed using Schrödinger software (Maestro 11.1.001). It is important to state that initially large library of hundred molecules was considered for virtual design. Finally, it was narrowed down to some interesting ones with considerable docking score and also keeping in mind their synthetic feasibility.

Molecular docking

Protein preparation

The available crystal structure of tankyrase1 in complex with IWR1 (PDB ID: 4OA7) [3] and PI3K (PDB ID: 3L54) [4] were downloaded from the protein databank (https://www.rcsb.org) both having the resolution of 2.30 Å. We selected the structure (PDB IDs: 4OA7 and 3L54) based on the best available resolution, R (free and work) values and the number of residues resolved. The ligand was

initially analyzed using the 'protein preparation wizard' module of Schrödinger software (Schrödinger's, LLC, New York, NY, USA). Initially, protein was present in tetrameric form later we converted it into monomeric form without further modification of the protein. During protein preparation, hydrogens were added, bond order was assigned, and missing loops and side chains were updated using prime. To avoid unnecessary hindrance during docking, water molecules were removed within 5 Å of hit groups. Later, protein selection was carried out by a standard docking protocol.

Receptor grid generation:

After protein preparation, the next step is to identify the binding pocket and generate the grid. While preparing the grid, it was made sure that the prepared protein is included in the workspace, i.e., to make sure that the circle next to the prepared molecule is highlighted and a 10 Å grid was generated around the ligand using the receptor grid generation of the glide module and applied standard parameters of the glide tool (Schrödinger's, LLC, New York, NY, USA).

Ligand preparation:

All the hundred molecules were drawn in ChemDraw and saved in a mole MDL SD file (sdf) along with the standard. After entering all entities, the ligand preparation was commanded and ionization states were generated at pH 7.0+/-2.0. Initially, an attempt was made to generate tautomers and later a maximum of thirty-two stereoisomers were generated for each tautomer using the OPLS3 2015 force field [5].

Ligand docking

The receptor grid and lip prep or prepared ligand were subjected to Glide XP docking using a standard protocol of glide (Schrödinger's, LLC, New York, NY, USA). Standard parameters were applied, including van der Wall radii scaling factor of 0.80 for nonpolar atoms with a partial charge cut-off of 0.15. The number of poses reported was ten per ligand. Per residue interactions, scores were calculated for residue within 5 Å of the grid center.

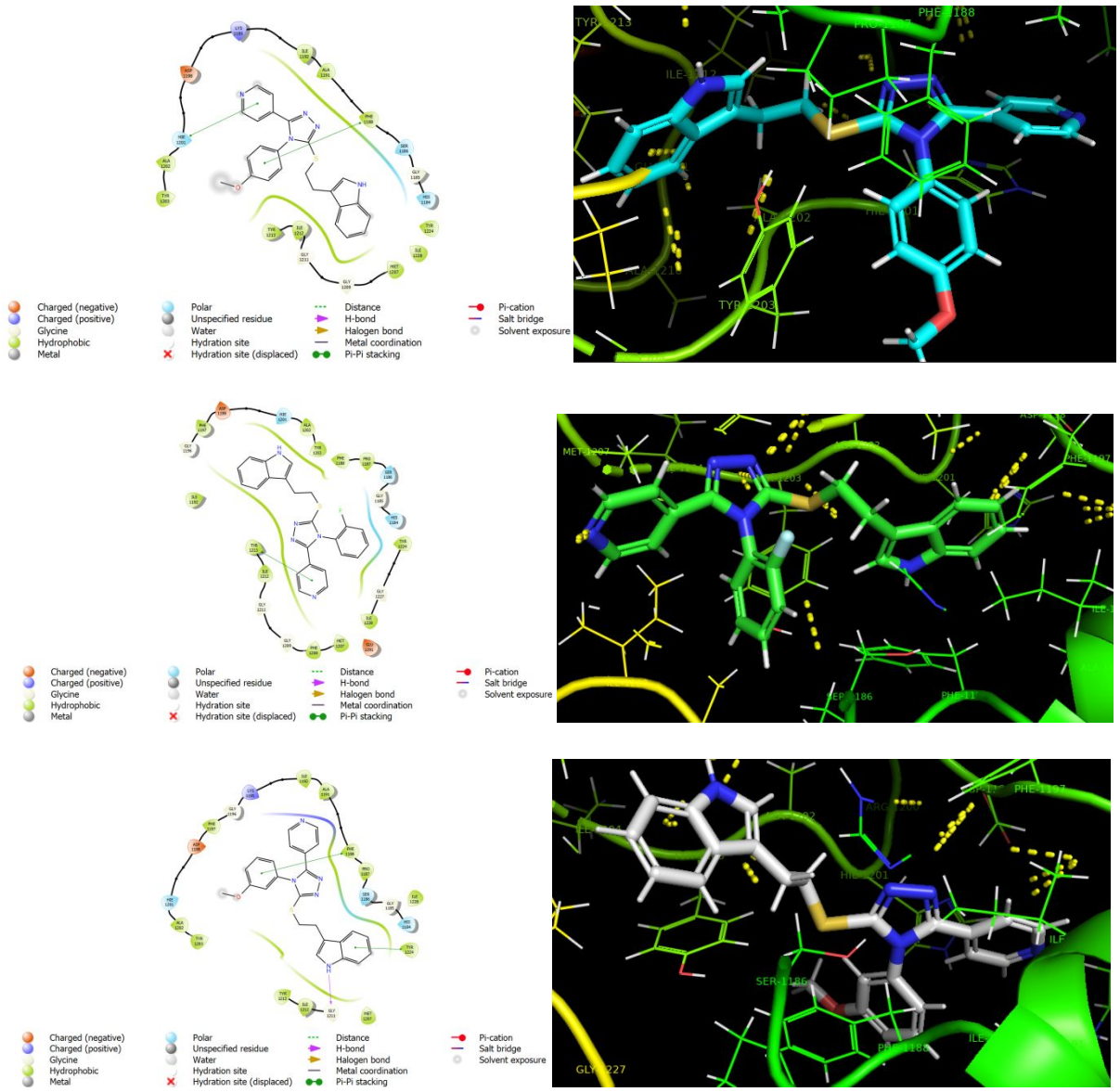

Figure S1: (**A**) Docking pose of **14a** in PDB ID 4OA7 is shown in a 2D structure pyridine was shown a Pi-Pi staking with HID 1201 and phenyl ring with PHE 1188 represented by green line; (**B**) Docking pose of **14n** in PDB ID 4OA7 are shown in a 2D structure where pyridine ring was shown Pi-Pi staking with TYR 1213 represented by green line; (**C**) Docking pose of **14q** in PDB ID 4OA7 is shown in a 2D structure phenyl was shown Pi-Pi staking with PHE 1188 and indole NH showing H-bond with GLY 1211 represented by the pink arrow.

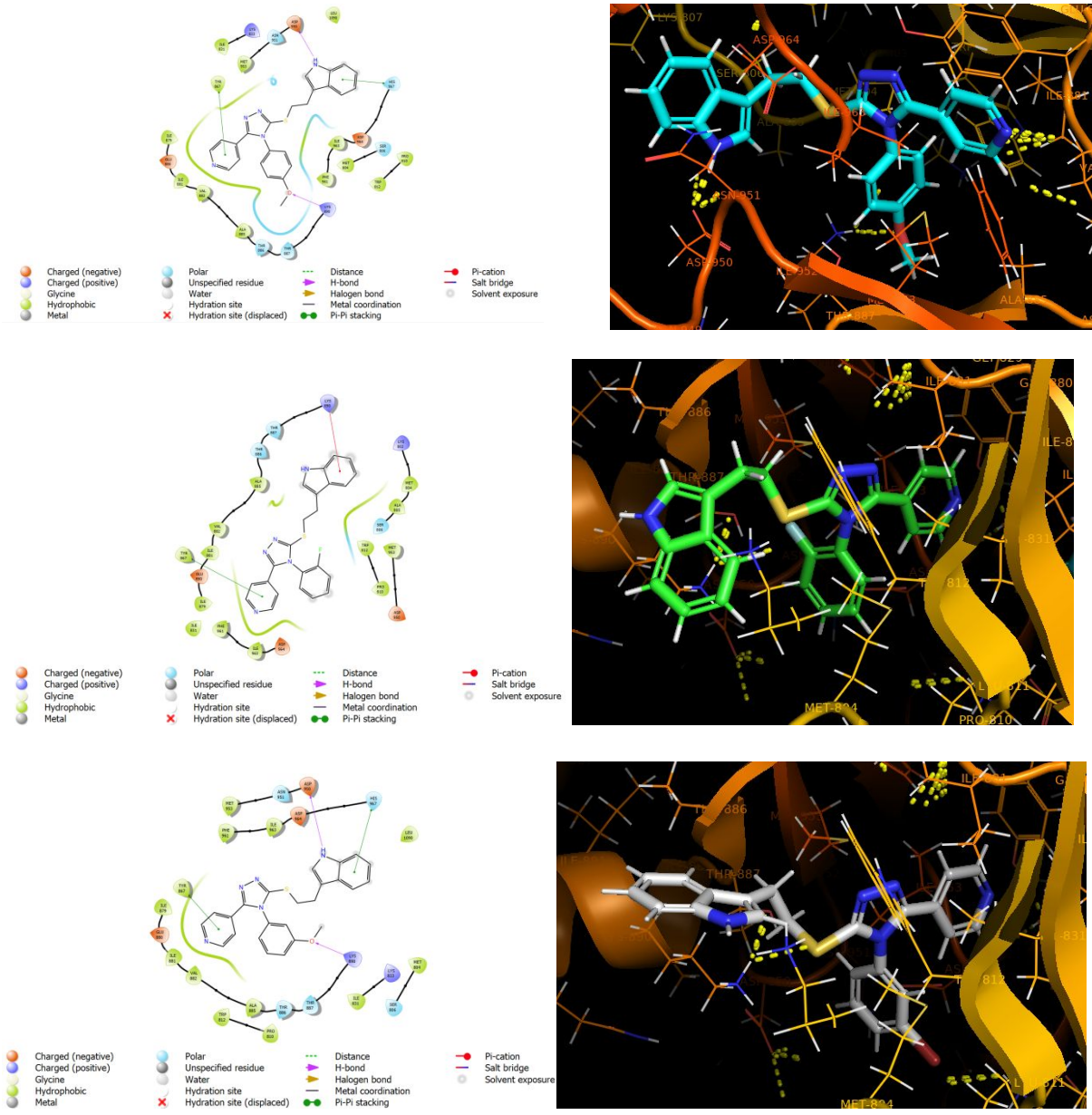

Figure S1. (**D**) Docking pose of **14a** in PDB ID 3L54 is shown in a 2D structure where indole NH was showing interaction with ASP 950 via H-bonding is represented by a pink arrow line and on other hand pyridine showing Pi-Pi staking with TYR 867 represented by green line; (**E**) Docking pose of **14n** in PDB ID 3L54 is shown in a 2D structure where indole interacts with LYS 890 via Pi-cation and represented by the red line. On the other hand, pyridine was showing Pi-Pi staking with TYR 867 represented by the green line; (**D**) Docking pose of **14n** in PDB ID 3L54 is shown in a 2D structure where indole interacts with LYS 890 & ASP 950 via H-bonding and represented by pink arrow. On the other hand, pyridine was showing Pi-Pi staking with TYR 867 & HIS 967 amino acid residue represented by the green line.

ADME property prediction

Seventeen hits were identified by using virtual screening and molecular docking studies, it was of our interest to look for the ADME properties of the identified compounds. Whether they showed

drug-like properties or not was the next question and examined the compliance with Lipinski's rule of five. There are various *in silico* tools available for predicting the pharmacokinetics of a molecule. QikProp module version 5.4 of Maestro, Schrodinger was used to calculate the molecular descriptor and predict the ADME profile of these synthesized compounds [6].

Chemistry

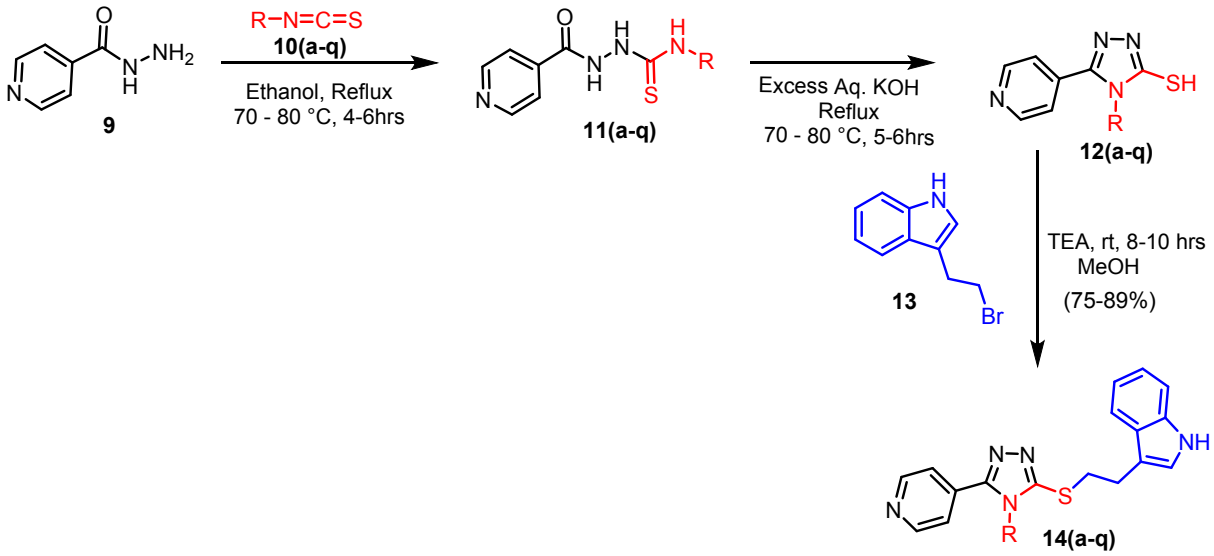

General procedure for the synthesis of 2-isonicotinoyl-N-phenylhydrazine-1-carbothioamide **(11a-q).**

Hydrazide **9** (0.5 g) is taken in absolute alcohol (5 mL) was charged with 1.2 equivalents of different isothiocyanates (**10a-q**) (aliphatic/ aromatic) were added and the reaction mixture was refluxed for 4-6 hrs [7]. After the completion of the reaction, observed by TLC, the reaction mixture was allowed to attain room temperature and poured onto crushed ice to form a colorless precipitate which was filtered, washed with cold alcohol and then dried under vacuum to yield the corresponding thiosemicarbazides (**11a-q**). These thiosemicarbazides were directly used in the next step with purification by column chromatography and **11a** was confirmed by ^{1}H NMR (500 MHz, DMSO–d_6) δ 11.69 (s, 1H), 9.95 (s, 1H), 9.66 (s, 1H), 8.16 (d, J = 10.0 Hz, 1H), 7.46 (dd, J = 8.0 Hz, J =5.0 Hz, 1H), 7.31 (d, J = 10.0 Hz, 2H), 7.19–7.12 (m, 2H), 6.88 (d, J = 10.0 Hz, 2H), 3.73 (s, 3H).

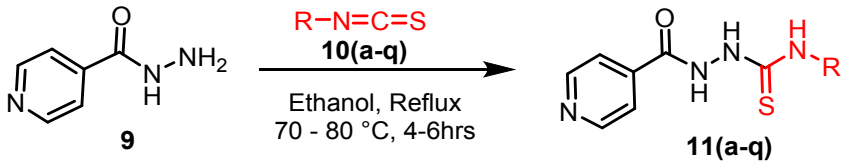

General procedure for the synthesis of 4-phenyl-5-(pyridin-4-yl)-4H-1,2,4-triazole-3-thiol (**12a-q).**

To the ethanolic solution of 0.1 g of 2-isonicotinoyl-N-phenylhydrazine-1-carbothioamide (thiosemicarbazide **11a-q**), 2N solution of KOH (10 mL) was added and subjected to reflux for 4-6 hrs. After the completion of the reaction, observed by TLC, the reaction mixture was brought to ambient temperature and poured onto crushed ice followed by acidification with 2N HCl to get the solid residue [8]. The solid precipitate was then filtered, washed with excess water, dried under vacuum and recrystallized in ethanol in order to get the corresponding pure 4-phenyl-5-(pyridin-4-yl)-4H-1,2,4-triazole-3-thiol compounds as a mixture of tautomer's (**12a-q).** Where **12a** was ^{1}H NMR (500 MHz, DMSO–d_6) δ 14.31 (s, 1H), 8.58 (dd, J = 5.0 Hz, 2H), 7.33 (d, J = 10.0 Hz, 2H), 7.25 (dd, J = 10.0 Hz, J =5.0 Hz, 2H), 7.06 (d, J = 15.0 Hz, 2H), 3.81 (s, 3H).

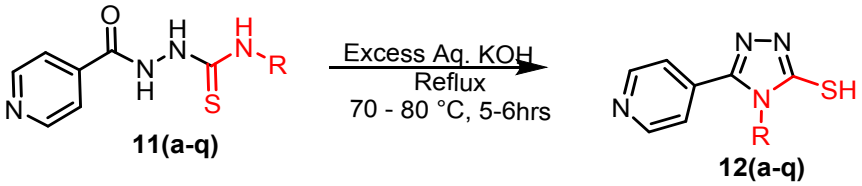

General procedure for the synthesis of 3-(2-((4-phenyl-5-(pyridin-4-yl)-4H-1,2,4-triazol-3-yl)thio)ethyl)-1H-indole **(14a-q).**

To the methanolic solution of (10 mL) 0.1 g of 4-phenyl-5-(pyridin-4-yl)-4H-1,2,4-triazole-3-thiol (**12a-q)** 1.2 equivalents of 3-(2-bromoethyl)-1H-indole **13** was added along with triethylamine (4 equivalent). The reaction mixture was stirred at ambient temperature for 8-10 hrs. After the completion of the reaction, observed by TLC, the reaction mixture was quenched with an excess of water (30 mL) and extracted with dichloromethane (3 x 20 mL). The combined organic layers were dried over anhydrous sodium sulphate, filtered, and evaporated under a vacuum to afford the crude product which was recrystallized in ethyl acetate/hexane to afford the pure target compounds **14a-q**.

During the experimental process, there is no unexpected or unusually high safety hazards were encountered.

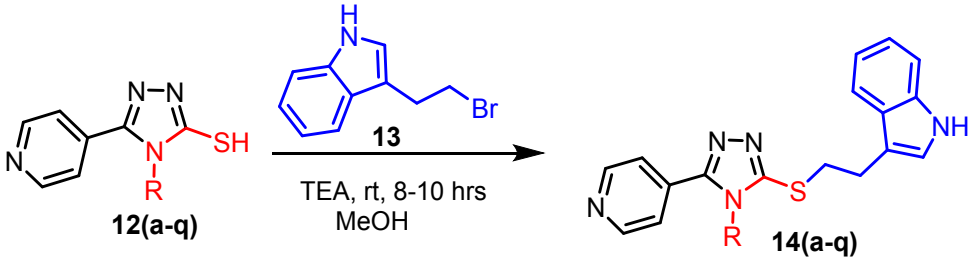

3-(2-((4-(4-methoxyphenyl)-5-(pyridin-4-yl)-4H-1,2,4-triazol-3-yl)thio)ethyl)-1H-indole (14a):

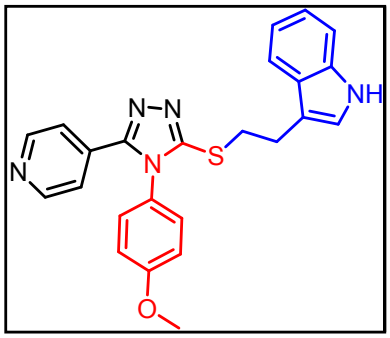

Light yellowish white solid 87% yield; Melting point 202.5 °C; ^{1}H NMR (400 MHz, DMSO–d_6) δ 10.85 (s, 1H), 8.58 (dd, *J* = 4.8 Hz, *J* = 1.6 Hz, 2H), 7.60 (d, *J* = 7.6 Hz, 1H), 7.39–7.33 (m, 5H), 7.18 (d, *J* = 2.0 Hz, 1H), 7.10–7.05 (m, 3H), 7.01–6.97 (m, 1H), 3.82 (s, 3H), 3.49 (t, *J* = 7.6 Hz, 2H), 3.15 (t, *J* = 7.6 Hz, 2H); ^{13}C NMR (100 MHz, DMSO–d_6) δ 151.9, 149.8, 136.7, 136.4, 133.1, 127.4, 126.2, 125.5, 123.5, 122.8, 121.5, 121.4, 120.7, 118.8, 117.0, 112.8, 112.3, 111.9, 102.2, 46.6, 34.2, 25.9; IR (KBr) υ 3252, 1600, 1511, 1439, 1337, 1298, 1254, 1209, 1173, 1125, 1015, 832, 797, 741, 695, 632 cm^{-1}; HRMS (ESI); *m/z* calcd for $C_{24}H_{21}N_5OS$ [M+2] 429.1623, found 429.1474.

3-(2-((4-butyl-5-(pyridin-4-yl)-4H-1,2,4-triazol-3-yl)thio)ethyl)-1H-indole (14b):

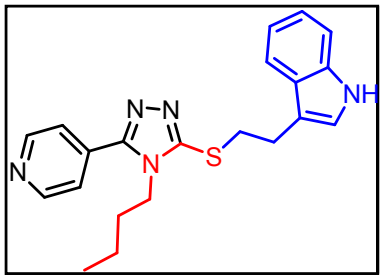

Light whitish yellow solid 72% yield; Melting point 182.7 °C; ^{1}H NMR (400 MHz, DMSO–d_6) δ 10.89 (s, 1H), 8.77 (dd, *J* = 4.8 Hz, *J* = 1.6 Hz, 2H), 7.71 (dd, *J* = 4.4 Hz, *J* = 1.6 Hz, 2H), 7.60 (d, *J* = 7.6 Hz, 1H), 7.35 (d, *J* = 8.0 Hz, 1H), 7.23 (d, *J* = 2.0 Hz, 1H), 7.08 (t, *J* = 6.8 Hz, 1H), 6.98 (t, *J* = 7.2 Hz, 1H), 3.99 (t, *J* = 7.2 Hz, 2H), 3.56 (t, *J* = 7.2 Hz, 2H), 3.17 (t, *J* = 7.6 Hz, 2H), 1.49 (p, *J* = 7.6 Hz, 2H), 1.10 (sex, *J* = 7.2 Hz, 2H), 0.73 (t, *J* = 7.6 Hz, 3H); ^{13}C NMR (100 MHz, DMSO–d_6) δ 153.2, 152.6, 150.9, 136.7, 135.3, 127.4, 123.6, 122.8, 121.5, 118.9, 118.8, 112.7, 111.9, 46.2, 44.5, 33.9, 31.6, 25.9, 19.4; IR (KBr) υ 3210, 2929, 1600, 1457, 1432, 1359, 1298, 1218, 1096, 818, 747, 741, 695, 688, 632 cm^{-1}; HRMS (ESI); *m/z* calcd for $C_{21}H_{23}N_5S$ [M+2] 379.1831, found 379.1686.

3-(2-((4-allyl-5-(pyridin-4-yl)-4H-1,2,4-triazol-3-yl)thio)ethyl)-1H-indole (14c):

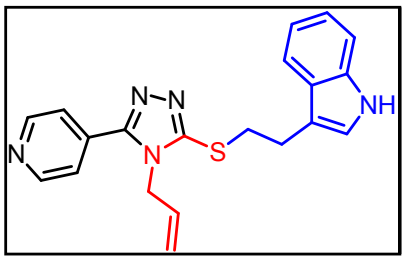

Light whitish yellow solid 79% yield; Melting point 195.4 ℃; ^{1}H NMR (400 MHz, DMSO–d_6) δ 10.88 (s, 1H), 8.75 (dd, *J* = 2.8 Hz, *J* = 1.6 Hz, 2H), 7.67 (dd, *J* = 4.8 Hz, *J* = 2.0 Hz, 2H), 7.60 (d, *J* = 8.0 Hz, 1H), 7.35 (d, *J* = 8.0 Hz, 1H), 7.22 (s, 1H), 7.08 (t, *J* = 7.6 Hz, 1H), 6.99 (t, *J* = 7.6 Hz, 1H), 5.99–5.91 (m, 1H), 5.22 (t, *J* = 10.8 Hz, 1H), 4.80 (d, *J* = 17.2 Hz, 1H), 4.66 (t, *J* = 4.0 Hz, 2H), 3.53 (t, *J* = 7.6 Hz, 2H), 3.16 (t, *J* = 7.2 Hz, 2H); ^{13}C NMR (100 MHz, DMSO–d_6) δ 153.3, 150.8, 136.6, 136.5, 134.8, 132.5, 127.3, 127.3, 123.6, 123.4, 122.5, 121.6, 119.0, 118.8, 117.6, 112.6, 111.9, 46.9, 34.1, 25.7; IR (KBr) υ 3417, 3392, 3217, 1598, 1435, 1346, 1205, 1012, 980, 917, 821, 745, 690, 623 cm^{-1}; HRMS (ESI); *m/z* calcd for $C_{20}H_{19}N_5S$ [M+2] 363.1518, found 363.1368.

3-(2-((4-(4-chlorophenyl)-5-(pyridin-4-yl)-4H-1,2,4-triazol-3-yl)thio)ethyl)-1H-indole (14d):

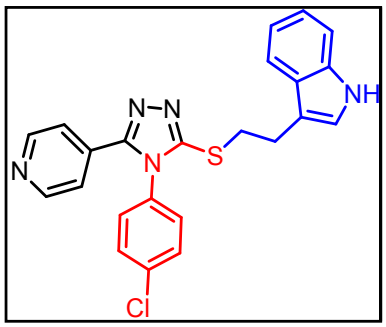

Light yellow solid 84% yield; Melting point 198.2 ℃; ^{1}H NMR (400 MHz, DMSO–d_6) δ 10.85 (s, 1H), 8.59 (dd, *J* = 4.8 Hz, *J* = 1.6 Hz, 2H), 7.64–7.58 (m, 3H), 7.50 (d, *J* = 8.0 Hz, 2H), 7.35–7.32 (m, 3H), 7.18 (s, 1H), 7.07 (t, *J* = 7.2 Hz, 1H), 6.99 (t, *J* = 7.2 Hz, 1H), 3.50 (t, *J* = 7.2 Hz, 2H), 3.14 (t, *J* = 7.2 Hz, 2H); ^{13}C NMR (100 MHz, DMSO–d_6) δ 154.0, 152.7, 150.6, 136.7, 135.5, 134.3, 132.9, 130.6, 130.1, 127.4, 123.5, 122.1, 121.5, 118.9, 118.8, 112.7, 111.9, 33.4, 25.7; IR (KBr) υ 3417, 2896, 1598, 1491, 1433, 1409, 1376, 1329, 1215, 1095, 1002, 832, 779, 747, 667, 623 cm^{-1}; MS (ESI); *m/z* calcd for $C_{23}H_{18}ClN_5S$ [M+H] 433.1050, found 433.0989.

3-(2-((5-(pyridin-4-yl)-4-(p-tolyl)-4H-1,2,4-triazol-3-yl)thio)ethyl)-1H-indole (14e):

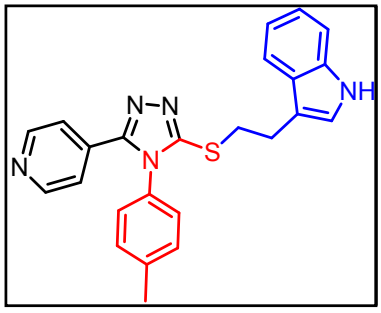

Light yellow solid 82% yield; Melting point 219.4 ℃; ^{1}H NMR (400 MHz, DMSO–d_6) δ 10.89 (s, 1H), 8.60 (dd, *J* = 4.8 Hz, *J* = 1.2 Hz, 2H), 7.63 (d, *J* = 8.0 Hz, 1H), 7.39–7.33 (m, 7H), 7.20 (d, *J* = 2.4 Hz, 1H), 7.10 (t, *J* = 7.2 Hz, 1H), 7.01 (t, *J* = 7.6 Hz, 1H), 3.53 (t, *J* = 7.2 Hz, 2H), 3.18 (t, *J* = 7.6 Hz, 2H), 2.41 (s, 3H); ^{13}C NMR (100 MHz, DMSO–d_6) δ 154.5, 152.9, 150.8, 140.9, 136.9, 134.7, 131.6, 131.3, 128.1, 127.6, 123.7, 122.2, 121.7, 119.1, 113.0, 112.1, 33.4, 26.0, 21.5; IR

(KBr) υ 3224, 2683, 1592, 1507, 1436, 1379, 1329, 1216, 1116, 1007, 820, 773, 742, 769, 701, 628, 623 cm^{-1}; HRMS (ESI); *m/z* calcd for $C_{24}H_{21}N_5S$ [M+2] 413.1674, found 413.1531.

3-(2-((4-ethyl-5-(pyridin-4-yl)-4H-1,2,4-triazol-3-yl)thio)ethyl)-1H-indole (14f):

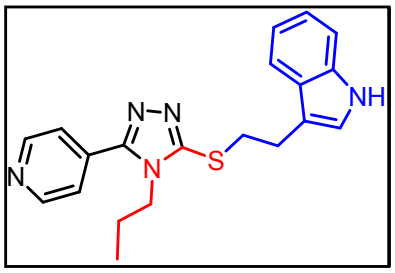

Light whitish yellow solid 75% yield; Melting point 181.3 ℃; ^{1}H NMR (400 MHz, DMSO–d_6) δ 10.89 (s, 1H), 8.77 (d, *J* = 5.2 Hz, 2H), 7.71 (d, *J* = 5.2 Hz, 2H), 7.60 (d, *J* = 8.0 Hz, 1H), 7.35 (d, *J* = 8.0 Hz, 1H), 7.23 (d, *J* = 1.6 Hz, 1H), 7.08 (t, *J* = 8.0 Hz, 1H), 6.98 (t, *J* = 7.2 Hz, 1H), 4.02 (q, *J* = 7.2 Hz, 2H), 3.56 (t, *J* = 7.6 Hz, 2H), 3.17 (t, *J* = 7.6 Hz, 2H), 3.09 (p, *J* = 7.6 Hz, 2H), 1.19 (t, *J* = 7.2 Hz, 3H); ^{13}C NMR (100 MHz, DMSO–d_6) δ 153.0, 152.4, 150.9, 136.7, 135.1, 127.4, 123.6, 122.8, 121.5, 118.9, 118.8, 112.7, 111.9, 46.2, 33.8, 25.9, 15.4, 9.0; IR (KBr) υ 3250, 2673, 1599, 1438, 1393, 1350, 1278, 1217, 1172, 1047, 964, 825, 772, 740, 665, 623 cm^{-1}; HRMS (ESI); *m/z* calcd for $C_{20}H_{21}N_5S$ [M+2] 365.1647, found 365.1529.

3-(2-((4-(3-bromophenyl)-5-(pyridin-4-yl)-4H-1,2,4-triazol-3-yl)thio)ethyl)-1H-indole (14g):

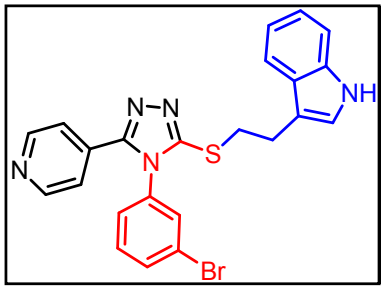

Light yellow solid 84% yield; Melting point 219.1 ℃; ^{1}H NMR (400 MHz, DMSO–d_6) δ 10.86 (s, 1H), 8.60 (d, *J* = 6.0 Hz, 2H), 7.82 (dd, *J* = 12.0 Hz, *J* = 6.0 Hz, 2H), 7.60 (d, *J* = 8.0 Hz, 1H), 7.53–7.47 (m, 2H), 7.34 (t, *J* = 6.0 Hz, 3H), 7.18 (s, 1H), 7.07 (t, *J* = 7.6 Hz, 1H), 6.99 (t, *J* = 7.6 Hz, 1H), 3.50 (t, *J* = 6.8 Hz, 2H), 3.15 (t, *J* = 7.2 Hz, 2H); ^{13}C NMR (100 MHz, DMSO–d_6) δ 153.9, 152.6, 150.6, 136.7, 135.4, 134.3, 133.9, 132.3, 131.0, 127.5, 127.4, 123.5, 122.7, 122.1, 121.5, 118.9, 118.8, 112.7, 111.9, 33.4, 25.7; IR (KBr) υ 3382, 3154, 3062, 2939, 2745, 2541 2216. 1922, 1645, 1611, 1569, 1512, 1465, 1344, 1282, 1239, 1137, 1055, 974, 885, 767, 622 cm^{-1}; HRMS (ESI); *m/z* calcd for $C_{23}H_{18}BrN_5S$ [M+3] 478.0710, found 478.0472.

3-(2-((4-(2,6-dimethylphenyl)-5-(pyridin-4-yl)-4H-1,2,4-triazol-3-yl)thio)ethyl)-1H-indole (14h):

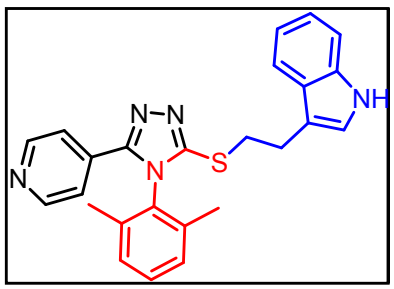

Light yellow solid 79% yield; Melting point 181.6 ℃; ^{1}H NMR (400 MHz, DMSO–d_6) δ 10.86 (s, 1H), 8.57 (d, *J* = 6.4 Hz, 2H), 7.64 (d, *J* = 7.6 Hz, 1H), 7.44 (t, *J* = 6.8 Hz, 1H), 7.34 (d, *J* = 6.0 Hz, 3H), 7.28 (d, *J* = 6.0 Hz, 2H), 7.18 (d, *J* = 2.0 Hz, 1H), 7.07

(t, J = 6.4 Hz, 1H), 6.99 (t, J = 7.6 Hz, 1H), 3.57 (t, J = 7.2 Hz, 2H), 3.18 (t, J = 7.6 Hz, 2H), 1.91 (s, 6H); ^{13}C NMR (100 MHz, DMSO–d_6) δ 153.9, 151.5, 151.1, 136.7, 135.9, 134.0, 131.9, 131.3, 129.9, 127.4, 123.5, 121.5, 120.1, 118.9, 112.7, 111.9, 32.4, 25.9, 17.6; IR (KBr) υ 3302, 3210, 1620, 1598, 1419, 1374, 1322, 1297, 1217, 1157, 981, 819, 778, 743, 660, 623 cm^{-1}; HRMS (ESI); *m/z* calcd for $C_{25}H_{23}N_5S$ [M+2] 427.1831, found 427.1682.

3-(2-((4-(2-bromophenyl)-5-(pyridin-4-yl)-4H-1,2,4-triazol-3-yl)thio)ethyl)-1H-indole (14i):

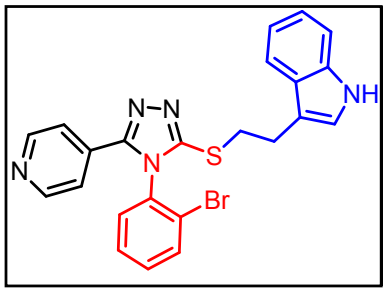

Light yellow solid 76% yield; Melting point 210.6 ℃; ^{1}H NMR (400 MHz, DMSO–d_6) δ 10.77 (s, 1H), 8.52 (d, J = 8.0 Hz, 2H), 7.66–7.58 (m, 2H), 7.51 (d, J = 8.0 Hz, 1H), 7.43 (t, J = 9.2 Hz, 1H), 7.36 (t, J = 8.0 Hz, 1H), 7.27–7.25 (m, 3H), 7.09 (s, 1H), 6.99 (t, J = 8.0 Hz, 1H), 6.90 (t, J = 7.6 Hz, 1H), 3.43 (t, J = 8.0 Hz, 2H), 3.05 (t, J = 7.6 Hz, 2H); ^{13}C NMR (100 MHz, DMSO–d_6) δ 157.7, 155.3, 154.2, 152.7, 150.6, 136.5, 133.8, 133.5, 130.4, 127.1, 126.4, 123.3, 121.2, 118.7, 118.6, 117.6, 117.4, 112.4, 111.7, 33.1, 25.5; IR (KBr) υ 3382, 3149, 3052, 2939, 2741, 2547, 2215, 1915, 1654, 1611, 1567, 1513, 1465, 1341, 1289, 1234, 1135, 1057, 970, 878, 763, 627 cm^{-1}; LC-MS (ESI); *m/z* calcd for $C_{23}H_{18}BrN_5S$ [M+3] 478.0701, found 478.0478.

3-(2-((4-(4-nitrophenyl)-5-(pyridin-4-yl)-4H-1,2,4-triazol-3-yl)thio)ethyl)-1H-indole (14j):

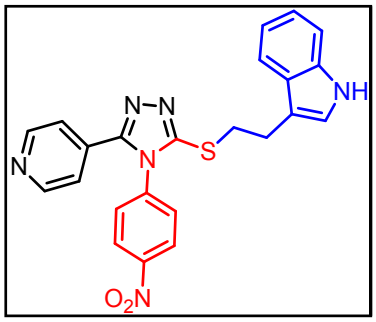

Yellow solid 75% yield; Melting point 224.5 ℃; ^{1}H NMR (400 MHz, DMSO–d_6) δ 10.80 (s, 1H), 8.57 (d, J = 6.0 Hz, 2H), 7.64 (dd, J = 8.0 Hz, J = 2.0 Hz, 1H), 7.59 (t, J = 3.6 Hz, 1H), 7.57–7.53 (m, 2H), 7.37 (dd, J = 5.2 Hz, J = 1.2 Hz, 1H), 7.35–7.31 (m, 3H), 7.15 (s, 1H), 7.06 (t, J = 6.8 Hz, 1H), 6.97 (t, J = 6.8 Hz, 1H), 3.48 (t, J = 7.2 Hz, 2H), 3.13 (t, J = 7.2 Hz, 2H); ^{13}C NMR (100 MHz, DMSO–d_6) δ 154.0, 152.6, 150.5, 136.6, 136.5, 135.0, 134.6, 134.3, 132.1, 131.1, 128.1, 127.3, 127.0, 123.5, 123.4, 122.3, 121.6, 119.0, 118.8, 112.6, 111.9, 33.5, 25.4; IR (KBr) υ 3398, 3385, 3157, 3062, 2931, 2742, 2541, 2214, 1915, 1644, 1605, 1561, 1505, 1461, 1343, 1282, 1234, 1125, 1052, 973, 872, 764, 621 cm^{-1}; MS (ESI); *m/z* calcd for $C_{23}H_{18}N_6O_2S$ [M+2] 444.1369, found 444.1224.

3-(2-((4-(4-fluorophenyl)-5-(pyridin-4-yl)-4H-1,2,4-triazol-3-yl)thio)ethyl)-1H-indole (14k):

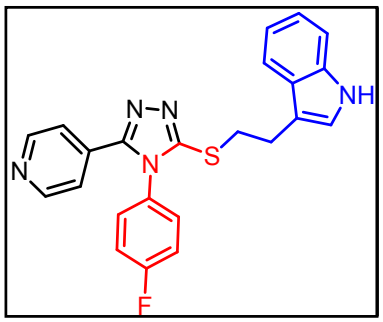

Light yellow solid 89% yield; Melting point 191.4 ℃; ^{1}H NMR (500 MHz, DMSO–d_6) δ 10.88 (s, 1H), 8.61 (d, *J* = 6.0 Hz, 2H), 7.74 (d, *J* = 2.0 Hz, 1H), 7.68 (d, *J* = 8.0 Hz, 1H), 7.61–7.57 (m, 2H), 7.48–7.46 (m, 1H), 7.35–7.33 (m, 3H), 7.19 (s, 1H), 7.08 (t, *J* = 7.5 Hz, 1H), 6.99 (t, *J* = 7.0 Hz, 1H), 3.50 (t, *J* = 7.5 Hz, 2H), 3.15 (t, *J* = 7.5 Hz, 2H); ^{13}C NMR (125 MHz, DMSO–d_6) δ 153.8, 152.6, 150.7, 136.7, 135.3, 134.5, 134.3, 132.1, 131.1, 128.3, 127.4, 127.2, 123.5, 122.1, 121.5, 118.9, 112.7, 111.9, 33.3, 25.8; IR (KBr) υ 3394, 3116, 3068, 2936, 2748, 2544, 2214, 1922, 1615, 1618, 1566, 1512, 1464, 1352, 1290, 1246, 1132, 1058, 982, 880, 778, 626 cm^{-1}; MS (ESI); *m/z* calcd for $C_{23}H_{18}FN_5S$ [M+H] 416.1345, found 416.1278.

3-(2-((4-(3-chlorophenyl)-5-(pyridin-4-yl)-4H-1,2,4-triazol-3-yl)thio)ethyl)-1H-indole (14l):

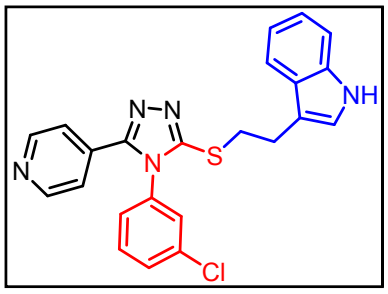

Light yellow solid 83% yield; Melting point 195.4 ℃; ^{1}H NMR (400 MHz, DMSO–d_6) δ 10.86 (s, 1H), 8.61 (dd, *J* = 4.8 Hz, *J* = 1.6 Hz, 2H), 7.72 (t, *J* = 2.0 Hz, 1H), 7.69–7.66 (m, 1H), 7.59 (dd, *J* = 6.4 Hz, *J* = 2.0 Hz, 2H), 7.47–7.44 (m, 1H), 7.35–7.32 (m, 3H), 7.18 (d, *J* = 6.0 Hz, 1H), 7.07 (t, *J* = 7.2 Hz, 1H), 6.99 (t, *J* = 7.2 Hz, 1H), 3.50 (t, *J* = 7.2 Hz, 2H), 3.15 (t, *J* = 7.6 Hz, 2H); ^{13}C NMR (100 MHz, DMSO–d_6) δ 154.0, 152.6, 150.5, 136.6, 136.5, 135.0, 134.6, 134.3, 132.1, 131.1, 128.1, 127.3, 127.0, 123.5, 123.4, 122.3, 121.6, 119.0, 118.8, 112.6, 112.6, 111.9, 111.9, 33.5, 25.4; IR (KBr) υ 3247, 2972, 2935, 2737, 2672, 2488, 1638, 1468, 1431, 1393, 1257, 1167, 1070, 1032, 802, 728, 692, 624 cm^{-1}; HRMS (ESI); *m/z* calcd for $C_{23}H_{18}ClN_5S$ [M+2] 433.1128, found 433.0989.

3-(2-((4-phenyl-5-(pyridin-4-yl)-4H-1,2,4-triazol-3-yl)thio)ethyl)-1H-indole (14m):

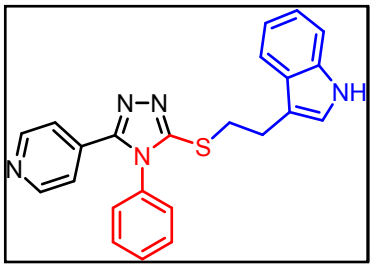

Light yellow solid 80% yield; Melting point 222.1 ℃; ^{1}H NMR (500 MHz, DMSO–d_6) δ 10.86 (s, 1H), 8.56 (dd, *J* = 5.0 Hz, *J* = 1.5 Hz, 2H), 7.62–7.55 (m, 4H), 7.47–7.45 (m, 2H), 7.35 (d, *J* = 1.5 Hz, 1H), 7.31 (dd, *J* = 4.5 Hz, *J* = 1.5 Hz, 2H), 7.19 (d, *J* = 2.0 Hz, 1H), 7.08 (t, *J* = 7.0 Hz, 1H), 6.99 (t, *J* = 8.0 Hz, 1H), 3.50 (t, *J* = 7.5 Hz, 2H), 3.15 (t, *J* = 8.0 Hz, 2H); ^{13}C NMR (125 MHz, DMSO–d_6) δ 154.1, 152.6, 150.6, 136.7, 134.5, 134.0, 130.9, 130.6, 128.1, 127.4, 123.5, 122.0, 121.5, 118.9, 112.7, 111.9, 33.2,

25.8; IR (KBr) υ 3291, 2217, 1597, 1495, 1434, 1377, 1338, 1271, 1218, 1122, 1008, 820, 797, 776, 755, 695, 664, 629 cm^{-1}; MS (ESI); *m/z* calcd for $C_{23}H_{19}N_5S$ [M+2] 399.1518, found 399.1372.

3-(2-((4-(2-fluorophenyl)-5-(pyridin-4-yl)-4H-1,2,4-triazol-3-yl)thio)ethyl)-1H-indole (14n):

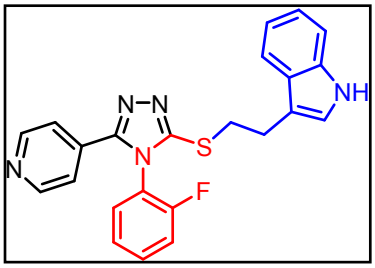

Light cream white solid 79% yield; Melting point 182.4 ℃; ^{1}H NMR (400 MHz, DMSO–d_6) δ 10.86 (s, 1H), 8.61 (d, *J* = 4.8 Hz, 2H), 7.75–7.66 (m, 2H), 7.60 (d, *J* = 8.0 Hz, 1H), 7.52 (t, *J* = 8.8 Hz, 1H), 7.44 (t, *J* = 7.6 Hz, 1H), 7.34 (t, *J* = 4.4 Hz, 3H), 7.17 (s, 1H), 7.08 (t, *J* = 7.2 Hz, 1H), 6.99 (t, *J* = 7.2 Hz, 1H), 3.51 (t, *J* = 7.2 Hz, 2H), 3.14 (t, *J* = 7.8 Hz, 2H); ^{13}C NMR (100 MHz, DMSO–d_6) δ 154.2, 152.7, 150.6, 136.5, 133.8, 133.6, 133.6, 130.4, 127.1, 126.4, 126.4, 123.3, 121.3, 121.3, 118.7, 118.6, 117.6, 117.4, 112.4, 111.7, 33.1, 25.5; IR (KBr) υ 3307, 1596, 1503, 1463, 1431, 1379, 1338, 1269, 1217, 1101, 1006, 862, 817, 751, 701, 655, 614 cm^{-1}; HRMS (ESI); *m/z* calcd for $C_{23}H_{18}FN_5S$ [M+2] 417.1424, found 417.1279.

3-(2-((5-(pyridin-4-yl)-4-(o-tolyl)-4H-1,2,4-triazol-3-yl)thio)ethyl)-1H-indole (14o):

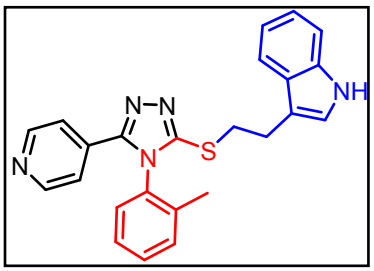

Light yellow solid 87% yield; Melting point 225.3 ℃; ^{1}H NMR (400 MHz, DMSO–d_6) δ 10.86 (s, 1H), 8.59 (dd, *J* = 4.8 Hz, *J* = 1.2 Hz, 2H), 7.63 (d, *J* = 8.0 Hz, 1H), 7.39–7.33 (m, 7H), 7.20 (d, *J* = 2.4 Hz, 1H), 7.10 (t, *J* = 7.2 Hz, 1H), 7.01 (t, *J* = 7.6 Hz, 1H), 3.53 (t, *J* = 7.2 Hz, 2H), 3.18 (t, *J* = 7.6 Hz, 2H), 2.41 (s, 3H); ^{13}C NMR (100 MHz, DMSO–d_6) δ 154.7, 153.1, 151., 141.1, 137.1, 134.9, 131.8, 131.5, 128.2, 127.8, 123.9, 122.3, 121.9, 119.3, 113.1, 112.3, 33.5, 26.1, 21.7; IR (KBr) υ 3224, 2683, 1592, 1507, 1436, 1379, 1329, 1216, 1116, 1007, 820, 773, 742, 769, 701, 628, 625 cm^{-1}; MS (ESI); *m/z* calcd for $C_{24}H_{21}N_5S$ [M+2] 413.1674, found 413.1539.

3-(2-((4-benzyl-5-(pyridin-4-yl)-4H-1,2,4-triazol-3-yl)thio)ethyl)-1H-indole (14p):

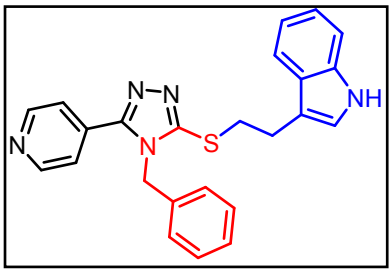

Light yellow solid 77% yield; Melting point 228.9 ℃; ^{1}H NMR (500 MHz, DMSO–d_6) δ 10.83 (s, 1H), 8.56 (dd, *J* = 4.5 Hz, *J* = 1.5 Hz, 2H), 7.58 (d, *J* = 8.0 Hz, 1H), 7.43 (t, *J* = 8.0 Hz, 1H), 7.32–7.30 (m, 3H), 7.16–7.03 (m, 5H), 6.97–6.94 (m, 2H), 3.72 (s, 2H), 3.46 (t, *J* = 7.0 Hz, 2H), 3.12 (t, *J* = 7.5 Hz, 2H); ^{13}C NMR (125 MHz, DMSO–d_6) δ 154.0, 152.4, 150.3, 140.4, 136.4, 134.2,

131.1, 130.8, 127.5, 127.1, 123.2, 121.6, 121.2, 118.6, 112.4, 111.6, 32.8, 25.4, 20.9; IR (KBr) υ 3397, 3392, 3154, 3064, 2903, 2739, 2542, 2217, 1921, 1645, 1609, 1561, 1512, 1452, 1346, 1286, 1238, 1131, 1054, 976, 875, 623 cm^{-1}; HRMS (ESI); *m/z* calcd for $C_{24}H_{21}N_5S$ [M+H] 413.1596, found 412.1527.

3-(2-((4-(3-methoxyphenyl)-5-(pyridin-4-yl)-4H-1,2,4-triazol-3-yl)thio)ethyl)-1H-indole (14q):

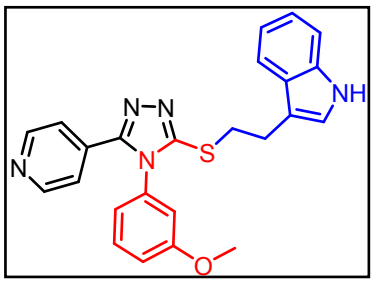

Light yellow solid 86% yield; Melting point 197.4 ℃; ^{1}H NMR (500 MHz, DMSO–d_6) δ 10.86 (s, 1H), 8.59 (dd, *J* = 4.5 Hz, *J* = 1.5 Hz, 2H), 7.61 (d, *J* = 8.0 Hz, 1H), 7.46 (t, *J* = 8.0 Hz, 1H), 7.36–7.33 (m, 3H), 7.19–7.12 (m, 3H), 7.07 (t, *J* = 7.0 Hz, 1H), 7.00–6.97 (m, 2H), 3.75 (s, 3H), 3.50 (t, *J* = 7.0 Hz, 2H), 3.15 (t, *J* = 7.5 Hz, 2H); ^{13}C NMR (125 MHz, DMSO–d_6) δ 160.6, 154.0, 152.6, 150.6, 136.7, 135.0, 134.5, 131.4, 127.4, 123.5, 121.9, 121.5, 120.1, 118.8, 116.4, 114.0, 112.8, 111.9, 56.1, 33.1, 25.7; IR (KBr) υ 3417, 3392, 3158, 3064, 2933, 2744, 2542, 2217, 1921, 1647, 1609, 1563, 1511, 1462, 1346, 1285, 1238, 1131, 1054, 976, 875, 769, 623 cm^{-1}; HRMS (ESI); *m/z* calcd for $C_{24}H_{21}N_5OS$ [M+2] 429.1623, found 429.1472.

Pharmacology

MTT assays

All the synthesized pyridine based 1,2,4-triazolo tethered indole conjugates (**14a-q**) were evaluated for their anti-proliferative activity using (3-4,5-dimethylthiazol-2-yl)-2,5-diphenyltetrazolium bromide (MTT) assay. The assay is based on the conversion of tetrazolium soluble salt into formazan crystals by the mitochondrial enzymes NAD and NADH–dehydrogenases. Colorectal adenocarcinoma (HCT-15 (ATCC-CCL-225™), HT-29 (ATCC-HTB-38™), DLD1 (ATCC- CCL-221™), and CaCO2, ATCC- HTB-37™), glioblastoma, brain cancer (A172, ATCC-CRL-1620™), teratocarcinoma, testicular cancer (TERA-1, ATCC- HTB-105™), and normal rat kidney cells NRK-52-E, ATCC-CRL-1571™ were plated at a density of 10,000 cells/well in a 96 well plate. After the cells attained normal morphology, cells were treated with the above conjugates at a single concentration of 10 µM for 24 hrs. The plate was placed at 37°C

in a humidified CO_2 incubator. Further, the supernatant was removed, and MTT solution at a concentration of 0.5 mg/mL was added, followed by incubation at 37 ˚C for 4 hrs in a humidified atmosphere. Subsequently, the media was removed, DMSO was added to dissolve the formazan crystals, and then the absorbance was recorded at 570 nm on i3x spectramax, molecular devices [11]. Compounds showing greater than 50% inhibition in the initial screening were further treated at varying doses of 10, 3.33, 1.11, 0.37, 0.12, and 0.041 µM concentrations. Cytotoxicity was expressed as the concentration of compounds that inhibit 50% cell proliferation (IC_{50}).

Cell cycle analysis

The effect of **14a, 14n** and **14q** on the cell cycle of the HT-29 cell line was evaluated by using flow cytometry at **14a** (1µM), **14n** (2µM) and **14q** (4µM) concentrations. These cells were seeded in a 6 well plate and kept in an incubator at 37°C for 24 hrs, and after attachment of cells with fully confluent, cells were treated with the test compounds. After treatment, cells were harvested and fixed overnight in 75% ice-cold ethanol at 4 ℃. Following PBS wash, fixed cells were pelleted and stained with RNase (50 U/mL) and PI (20µg/mL) solution for 20 mins at dark and room temperature. Further, the cells were analyzed by using flow cytometry [12].

Evaluation of mitochondrial membrane potential (MMP)

JC-1 staining method was used to study the effect of **14a, 14n** and **14q** on mitochondrial membrane potential (Δψm) of HT-29 cells. It was assessed by JC-1 dye, a specific mitochondrial fluorescent probe. Normally Δψm JC-1, form aggregates with high red fluorescence intensity so that a loss in the Δψm is indicated by a decrease in the red fluorescence and an increase in green fluorescence due to the shifting of dye from aggregate to monomeric form. JC-1 dye was used at a concentration of 2µM after seeding and treating HT-29 cells in a 6 well plate after incubation for 30mins in an incubator. The red/green fluorescence ratio serves as an indicator of Δψm loss [13].

Evaluation of apoptosis by Annexin V/ Propidium iodide (PI)

Annexin V is a very sensitive dye used to detect cellular apoptosis, while PI detects late apoptotic or necrotic population that is characterized by loss of integrity of nuclear and plasma membrane. HT-29 cells were plated in a 6 well plate, and after attaining morphology and desired cell density, treatment was given for 24 hrs. Further cells were harvested and washed in ice-cold PBS and

resuspended in an annexin binding buffer. Annexin-V-FITC and PI were used to stain the cells for 5-15mins following cell analysis by flow cytometry [14].

Evaluation of total reactive oxygen species (ROS)

The effect of **14a** (1μM), **14n** (2μM) and **14q** (4μM) on the production of total reactive oxygen species has been evaluated in the HT-29 colon cell line. HT-29 cells were plated in 6 well plate and after subsequent treatment, the plate was incubated with CM-H2DCFDA (2′,7′-dichlorodihydrofluorescein diacetate). Sigma Aldrich at a concentration of 5μM for 20 min at 37 °C. Post incubation of the dye, cells were washed with PBS followed by trypsinization with 0.25% trypsin. Then percentage intracellular ROS generation was measured using flow cytometry (Attune NXT, Thermo Fisher Scientific), 10,000 events were acquired for each treatment group [15].

Evaluation of Mitochondrial ROS

MitoSOX™ Red reagent was used to measure superoxide levels in live cells. MitoSOX™ Red is a novel fluorogenic dye that explicitly targets the mitochondrial membrane and upon oxidation, produces red fluorescence. HT-29 cells were plated in a 6 well plate and post-treatment incubated with 5μM MitoSOX™ Red for 1hr at 37°C in an incubator. Following incubation, cells were washed and trypsinized, 10,000 events were run in flow cytometry (Attune NXT, Thermo Fisher Scientific), and mean fluorescence intensity was measured [16].

Immunocytochemistry (ICC)

HT-29 cells were plated on poly D-lysine coated coverslips in a 6 well culture plate at a density of $2x10^6$ cells per well. Upon treatment with test compounds, cells were washed with PBS, fixed with 4% paraformaldehyde, and then permeabilized with 0.2% Triton X-100. Cells were blocked with 5% normal goat serum (NGS), washed, and incubated overnight with primary antibodies: β-Catenin (1:200 dilution), TAB-182 (1:200 dilution), NF-κB (1:800 dilution), PI3K-P85 (1:200 dilution) at 4ºC overnight incubation. Next, cells were washed with PBS and then incubated with secondary antibodies, namely Alexa Flour™ 488 goat anti-rabbit IgG (H+L) ActinGreen and Phalloidin Red, which were added to the cells for 15 min following PBS washing and mounting. Subsequently, nuclei were stained with Vectashield mounting medium for fluorescence with 4′,6-dia-midino-2-phenylindole (DAPI) (Cat no. H-1200, Vector Laboratories, Burlingame, CA). The

exclusion of the primary antibody prepared negative control slides. Slides were kept in a cool place until observed under oil emersion at 63x magnifications with a confocal microscope [17].

Western blot studies

HT-29 cells treated with compounds **14a, 14n** and **14q** were lysed after 72 h of incubation period with 2X SDS lysis buffer containing 0.5 M Tris-HCl, pH 6.8, glycerol, 10 % (w/v) SDS, protease inhibitor cocktail. The lysates were sonicated and centrifuged at 16000 g for 20 min following which supernatant was collected and subjected to protein estimation by Pierce TM BCA assay kit (ThermoFisher). 30 µg of proteins were separated on SDS gel and transferred to PVDF membranes. Membranes were exposed to a blocking buffer containing 5 % skim milk and probed with specific primary antibodies at 4 ℃ overnight. The primary antibodies used were as follows: APC (1:1000), PI3K p85 (phosphoinositide 3-kinase) (1:1000), p-PI3K p85 (1:1000), p-Pan-akt (1:1000), Pan-akt (1:1000), β-actin (1:1000), AXIN-1 (1:1000), AXIN-2 (1:1000), TAB-182 (tankyrase) (1:1000) P-GSK3β (1:1000), GSK3β (1:1000) and β-catenin (1:1000). Next, the blots were washed three times for 5 minutes with tris buffer solution with tween-20 (TBST) and incubated with HRP-conjugated secondary antibody for 1 h. The blots were washed three times with 1x TBST and the bands were detected by ECL Elistar ETA ultra 20 (Cyanagen) [18].

Molecular Dynamics (MD) simulation studies

MD simulations were carried out in flare using Schrödinger's software (Schrödinger's, LLC, New York, NY, USA). MD simulation determines the physical movements of molecules and atoms in the protein-ligand molecular docking complex [19]. The MD simulation was performed on the docked complex of compound **15r** with tankyrase1 and PI3K gamma protein (PDB ID: 4OA7 & 3L54) [41,42]. Before performing the MD simulation, the protein is critically vetted for any missing residues using the structure check wizard tool. Ligand energies were minimized using the OPLS3e force field [22]. Later, the 'Desmond' program was opened to start the system building and the protein structure was solvated using the PI3TP water model.

Protein was placed in the center of the orthorhombic box by using minimized volume where the distance between any atom of the solute and the edge of the solvent box was at least 10Å. Counter ions were added to neutralize the system and the salt ion concentration was set at 0.15M based on the psychological strength. After adding all the parameters, it started to run the job using a standard

protocol for system building (Desmond version). Following the energy minimization, a Nose-Hoover chain thermostat was used to carry out the NPT equilibration at 310 K to maintain a constant temperature. Additionally, a Martyn-Tobias-Klein barostat was employed to maintain a pressure of 1 bar [23]. MD simulations were carried out with the default settings of the normal calculation method, having the following parameters: simulation length was 10 ns, and the solvent model was an explicit method. The periodic boundary conditions were taken into consideration while performing MD simulations to avoid edge effects. The energy of the protein-ligand complex was minimized to 0.25 kcal/mol. After the MD simulation was completed, the trajectory was examined for RMSD and RMSF plots as well as protein-ligand contacts.

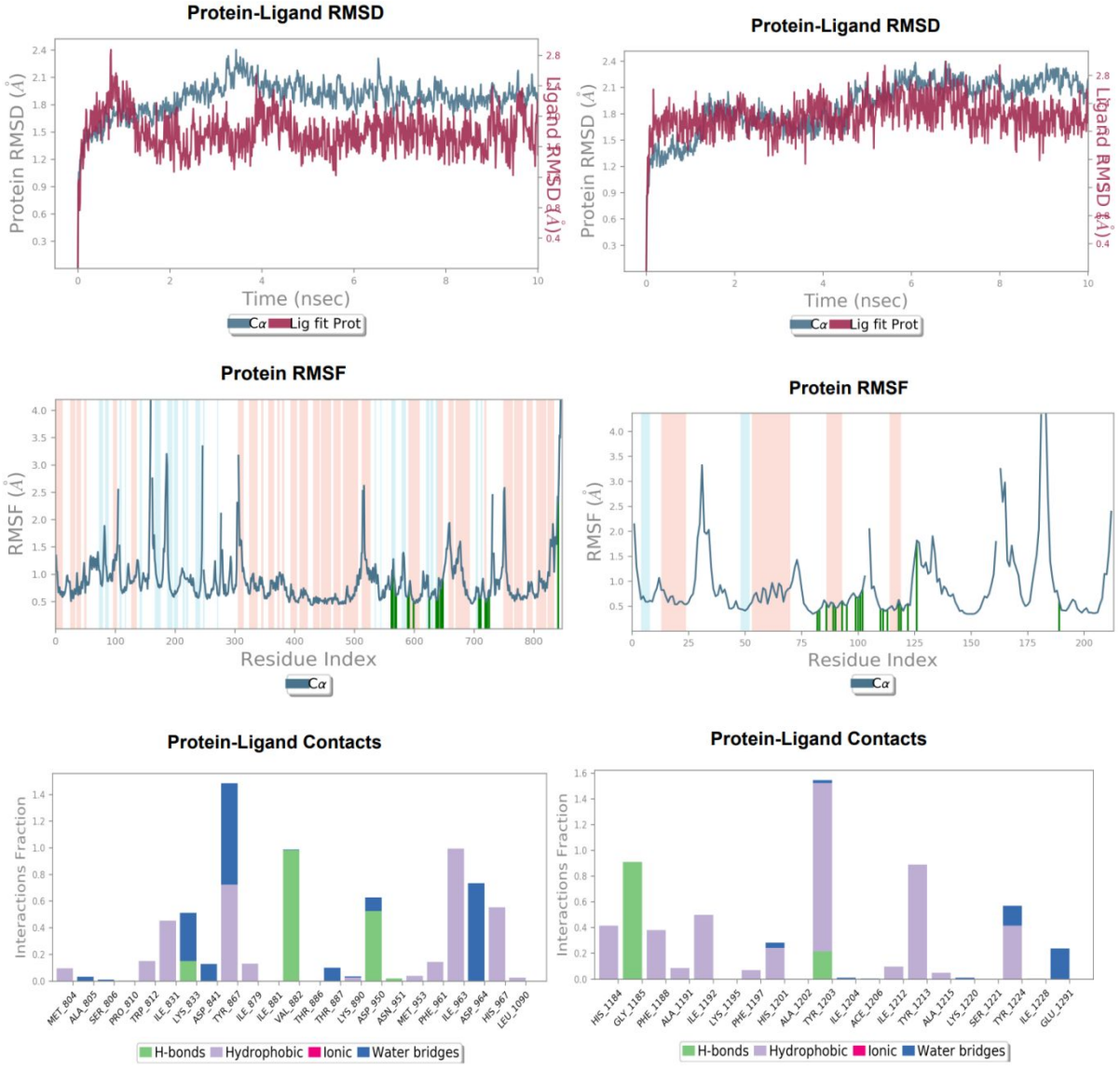

Figure S2. (**A**) Illustration of the MD trajectory analysis plots for 3L54 protein and **14a** ligand complex root mean square deviation (RMSD) for backbone atoms. (**B**) Analysis plots for 4OA7 protein and **14a** ligand complex root mean square deviation (RMSD) for backbone atoms. (C) The RMSF profile 3L54 protein with **14a** ligand representing local changes along the protein chain throughout the simulation trajectory. (**D**) The RMSF profile 4OA7 protein with **14a** ligand representing local changes along the protein chain throughout the simulation trajectory. (**E**) Plot representing protein-ligand interaction of **14a** with different residues of 3L54 throughout the simulation trajectory. (**F**) Protein-ligand interaction of **14a** with different residues of 4OA7 throughout the simulation trajectory.

Binding free energy calculation (MM-GBSA)

The complex's binding free energy was computed using the Molecular Mechanics with Generalised Born and Surface Area Solvation (MM-GBSA) technique. The protein-ligand binding free energy in a solvent is calculated as given below [24].

$\Delta G_{binding} = G_{complex} - (G_{protein} + G_{ligand})$ …….. (I)

Where $\Delta G_{binding}$ = free energy of binding, $G_{complex}$ = energy of complex, $G_{protein}$ = energy of protein, G_{ligand} = energy of ligand.

$G_x = E_{MM} + G_{solvation} - T\Delta S_{MM}$..... (II)

Where, Gx = receptor or ligand or receptor-ligand complex, E_{MM} = Molecular mechanics potential energy in a vacuum, $G_{solvation}$ = free energy of solvation, TS entropic contribution of the free energy in a vacuum, T and S represent the temperature and entropy.

$E_{MM} = E_{bonded} + E_{vwd} + E_{elec}$ ……..…… (III)

Where E_{MM} is bonded and non-bonded interactions energy, E_{bonded} = bonded energy, $E_{non\text{-}bonded}$ = non-bonded energy, E_{vwd} = van der Waals interaction energy, E_{elec} electrostatic energy.

$G_{solvation} = G_{polar} + G_{nonpolar}$ ……. (IV)

Where, G_{polar} = free energy of polar interactions, $G_{nonpolar}$ = free energy of nonpolar interactions.

The MM-GBSA method has been widely used to investigate biologically relevant systems. The binding free energy on the ensemble of structures created by Schrödinger's software (Schrödinger's, LLC, New York, NY, USA) was computed using the prime_mmgbsa tools [25]. The contribution of the entropic term is not included in the current implementation of the MM-GBSA within prime_mmgbsa. As previously demonstrated, the net entropy contribution is frequently minimal and exhibits substantial fluctuation (standard error) when compared to the other energy terms discussed above. The free energy of binding was computed for the entire 100-ns simulation time using structures stored every 100 ps.

General

All the computational studies like molecular modeling, virtual screening, MM-GBSA, ADMET analysis and molecular dynamics simulation were carried out by Maestro version 11.4 Schrödinger's software (Schrödinger's, LLC, New York, NY, USA). All the reagents, chemicals and antibodies utilized in this study were procured from GLR, Merck (India), and Sigma Aldrich, which were analytical reagent (AR) grades. TLC plates were of 0.25 mm silica gel 60-F254 that were used to monitor the reactions. In the UV cabinet, UV light was employed for the visualization spots in the reaction mixture. 1H and 13C NMR spectra were determined using the Bruker NMR (400 MHz and 100 MHz) and (500 MHz and 125 MHz) spectrometer. Chemical shifts are expressed as ppm against TMS internal reference and spectra were interpreted using the topspin software. Using Agilent mass spectrometry, the mass spectra including HRMS were recorded on ESI-MS, whereas IR spectra were recorded on Bruker ALPHA FT-IR spectrometer (Germany). Melting points of all synthesized compounds were measured using Buchi labortechnik AG 9230 automated melting point apparatus (Switzerland). All the final compounds prepared in this paper are new and confirmed with spectral data analysis. All the synthesized compounds were recrystallized in methanol and purified by column chromatography using basic alumina. Similarly, other reagents used include 3-(4,5-dimethylthiazol-2-yl)-2,5-diphenyltetrazolium bromide (MTT) reagent (Cat no: M2128), normal goat serum (Cat no: 5425), anti-rabbit IgG (Cat no: 7074S), anti-mouse IgG (Cat no: 7076S) were used for the *in-vitro* studies.

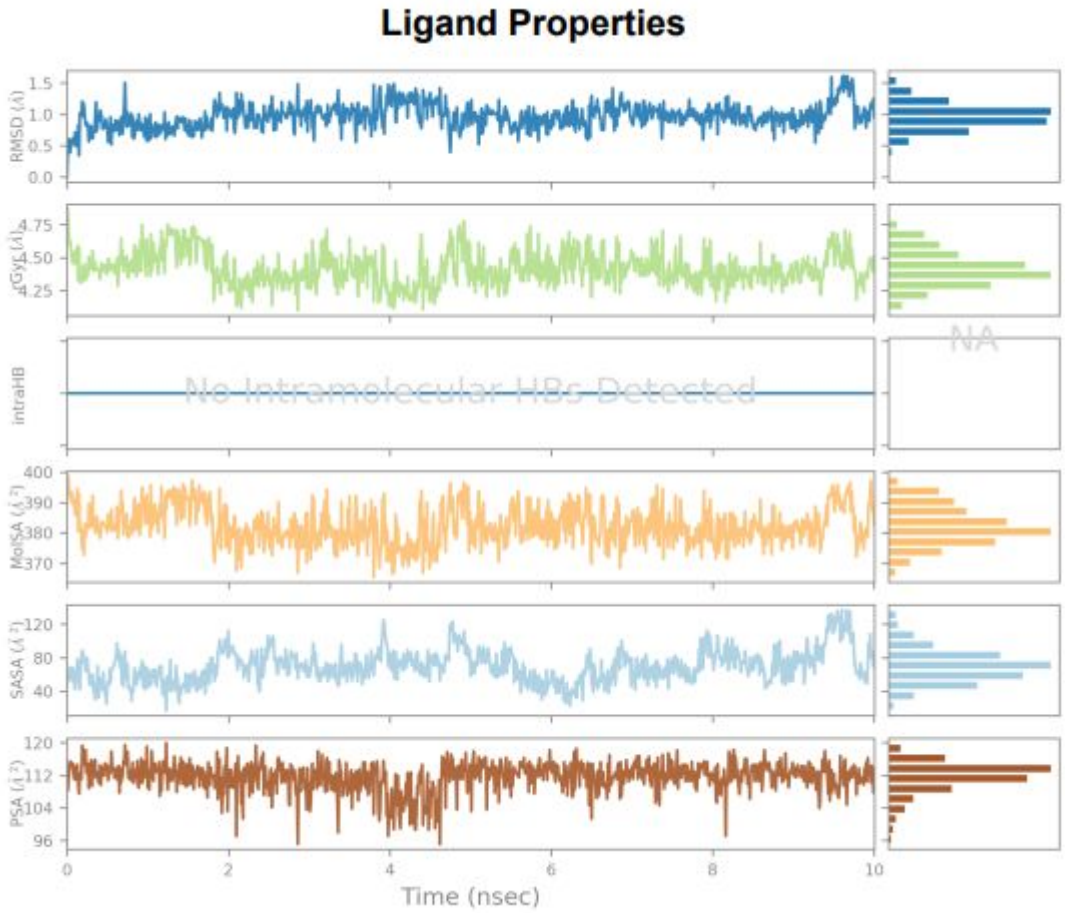

Figure S3. (**A**)Illustration of the MD trajectory analysis plots for 3L54 protein and **14a** ligand complex root mean square deviation (RMSD) for backbone atoms, RMSF profile 3L54 protein with **14a** ligand representing local changes along the protein chain throughout the simulation trajectory, Plot representing protein-ligand interaction of **14a** with different residues of 3L54 throughout the simulation trajectory. Radius of Gyration (rGyr), Intramolecular Hydrogen Bonds (intraHB), Molecular Surface Area (MolSA), Solvent Accessible Surface Area (SASA) and Polar Surface Area (PSA)

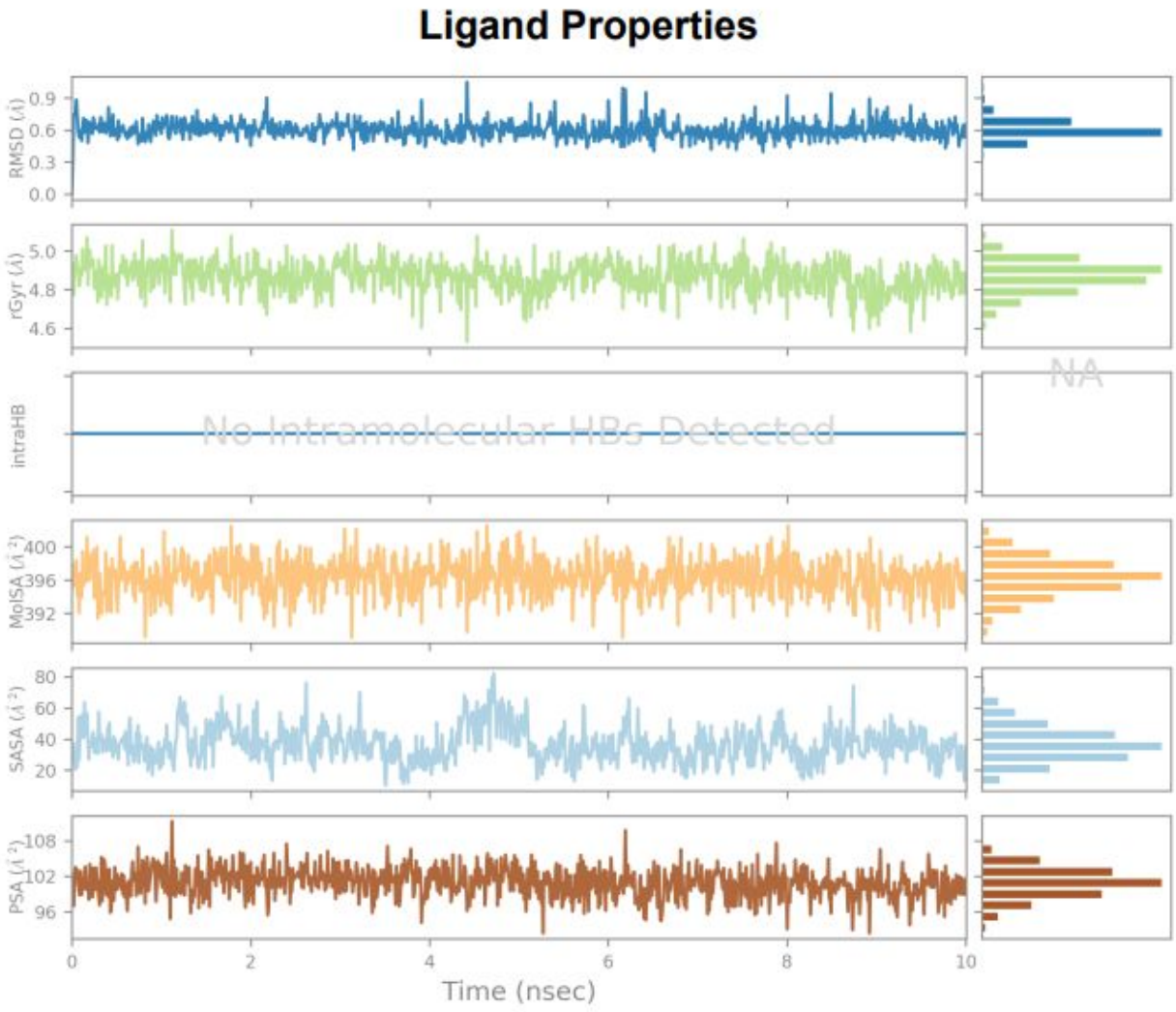

Figure S3. (**B**) Illustration of the MD trajectory Analysis plots for 4OA7 protein and **14a** ligand complex root mean square deviation (RMSD) for backbone atoms. The RMSF profile 4OA7 protein with **14a** ligand representing local changes along the protein chain throughout the simulation trajectory. Protein-ligand interaction of **14a** with different residues of 4OA7 throughout the simulation trajectory. Radius of Gyration (rGyr), Intramolecular Hydrogen Bonds (intraHB), Molecular Surface Area (MolSA), Solvent Accessible Surface Area (SASA) and Polar Surface Area (PSA)

Reference

(1) Aggarwal, R.; Sumran, G. An Insight on Medicinal Attributes of 1,2,4-Triazoles. *Eur. J. Med. Chem.* **2020**, *205*, 112652. https://doi.org/10.1016/J.EJMECH.2020.112652.

(2) Sterling, T.; Irwin, J. J. ZINC 15 - Ligand Discovery for Everyone. *J. Chem. Inf. Model.* **2015**, *55* (11), 2324–2337. https://doi.org/10.1021/ACS.JCIM.5B00559/ASSET/IMAGES/LARGE/CI-2015-00559J_0005.JPEG.

(3) Kulak, O.; Chen, H.; Holohan, B.; Wu, X.; He, H.; Borek, D.; Otwinowski, Z.; Yamaguchi, K.; Garofalo, L. A.; Ma, Z.; Wright, W.; Chen, C.; Shay, J. W.; Zhang, X.; Lum, L. Disruption of Wnt/β-Catenin Signaling and Telomeric Shortening Are Inextricable Consequences of Tankyrase Inhibition in Human Cells. *Mol. Cell. Biol.* **2015**, *35* (14), 2425–2435. https://doi.org/10.1128/mcb.00392-15.

(4) Knight, S. D.; Adams, N. D.; Burgess, J. L.; Chaudhari, A. M.; Darcy, M. G.; Donatelli, C. A.; Luengo, J. I.; Newlander, K. A.; Parrish, C. A.; Ridgers, L. H.; Sarpong, M. A.; Schmidt, S. J.; Van Aller, G. S.; Carson, J. D.; Diamond, M. A.; Elkins, P. A.; Gardiner, C. M.; Garver, E.; Gilbert, S. A.; Gontarek, R. R.; Jackson, J. R.; Kershner, K. L.; Luo, L.; Raha, K.; Sherk, C. S.; Sung, C. M.; Sutton, D.; Tummino, P. J.; Wegrzyn, R. J.; Auger, K. R.; Dhanak, D. Discovery of GSK2126458, a Highly Potent Inhibitor of PI3K and the Mammalian Target of Rapamycin. *ACS Med. Chem. Lett.* **2010**, *1* (1), 39–43. https://doi.org/10.1021/ml900028r.

(5) Rathod, B.; Chak, S.; Patel, S.; Shard, A. Tumor Pyruvate Kinase M2 Modulators: A Comprehensive Account of Activators and Inhibitors as Anticancer Agents. *RSC Med. Chem.* **2021**, *12* (7), 1121–1141. https://doi.org/10.1039/D1MD00045D.

(6) Lucas, A. J.; Sproston, J. L.; Barton, P.; Riley, R. J. Estimating Human ADME Properties, Pharmacokinetic Parameters and Likely Clinical Dose in Drug Discovery. *Expert Opin. Drug Discov.* **2019**, *14* (12), 1313–1327. https://doi.org/10.1080/17460441.2019.1660642.

(7) Naaz, F.; Ahmad, F.; Lone, B. A.; Khan, A.; Sharma, K.; Intzarali; Shaharyar, M.; Pokharel, Y. R.; Shafi, S. Apoptosis Inducing 1,3,4-Oxadiazole Conjugates of Capsaicin: Their in Vitro Antiproliferative and in Silico Studies. *ACS Med. Chem. Lett.* **2021**, *12* (11), 1694–1702. https://doi.org/10.1021/acsmedchemlett.1c00304.

(8) Naaz, F.; Ahmad, F.; Lone, B. A.; Pokharel, Y. R.; Fuloria, N. K.; Fuloria, S.; Ravichandran, M.; Pattabhiraman, L.; Shafi, S.; Shahar Yar, M. Design and Synthesis of Newer 1,3,4-

Oxadiazole and 1,2,4-Triazole Based Topsentin Analogues as Anti-Proliferative Agent Targeting Tubulin. *Bioorg. Chem.* **2020**, *95*. https://doi.org/10.1016/j.bioorg.2019.103519.

(9) Pedada, S. R.; Yarla, N. S.; Tambade, P. J.; Dhananjaya, B. L.; Bishayee, A.; Arunasree, K. M.; Philip, G. H.; Dharmapuri, G.; Aliev, G.; Putta, S.; Rangaiah, G. Synthesis of New Secretory Phospholipase A2-Inhibitory Indole Containing Isoxazole Derivatives as Anti-Inflammatory and Anticancer Agents. *Eur. J. Med. Chem.* **2016**, *112*, 289–297. https://doi.org/10.1016/j.ejmech.2016.02.025.

(10) Namballa, H. K.; Anchi, P.; Lakshmi Manasa, K.; Soni, J. P.; Godugu, C.; Shankaraiah, N.; Kamal, A. β-Carboline Tethered Cinnamoyl 2-Aminobenzamides as Class I Selective HDAC Inhibitors: Design, Synthesis, Biological Activities and Modelling Studies. *Bioorg. Chem.* **2021**, *117*. https://doi.org/10.1016/J.BIOORG.2021.105461.

(11) Yakkala, P. A.; Panda, S. R.; Shafi, S.; Naidu, V. G. M.; Yar, M. S.; Ubanako, P. N.; Adeyemi, S. A.; Kumar, P.; Choonara, Y. E.; Radchenko, E. V.; Palyulin, V. A.; Kamal, A. Synthesis and Cytotoxic Activity of 1,2,4-Triazolo-Linked Bis-Indolyl Conjugates as Dual Inhibitors of Tankyrase and PI3K. *Molecules* **2022**, *27* (21), 7642. https://doi.org/10.3390/MOLECULES27217642.

(12) Ahmed, S.; Kwatra, M.; Ranjan Panda, S.; Murty, U. S. N.; Naidu, V. G. M. Andrographolide Suppresses NLRP3 Inflammasome Activation in Microglia through Induction of Parkin-Mediated Mitophagy in in-Vitro and in-Vivo Models of Parkinson Disease. *Brain. Behav. Immun.* **2021**, *91*, 142–158. https://doi.org/10.1016/j.bbi.2020.09.017.

(13) Sakamuru, S.; Attene-Ramos, M. S.; Xia, M. Mitochondrial Membrane Potential Assay. *Methods Mol. Biol.* **2016**, *1473*, 17–22. https://doi.org/10.1007/978-1-4939-6346-1_2.

(14) Rieger, A. M.; Barreda, D. R. Accurate Assessment of Cell Death by Imaging Flow Cytometry. *Methods Mol. Biol.* **2016**, *1389*, 209–220. https://doi.org/10.1007/978-1-4939-3302-0_15.

(15) Wang, Q.; Zou, M. H. Measurement of Reactive Oxygen Species (ROS) and Mitochondrial ROS in AMPK Knockout Mice Blood Vessels. In *Methods in Molecular Biology*; Humana Press Inc., 2018; Vol. 1732, pp 507–517. https://doi.org/10.1007/978-1-4939-7598-3_32.

(16) Zorov, D. B.; Juhaszova, M.; Sollott, S. J. Mitochondrial Reactive Oxygen Species (ROS) and ROS-Induced ROS Release. *Physiol Rev* **2014**, *94*, 909–950.

https://doi.org/10.1152/physrev.00026.2013.-Byproducts.

(17) Ahmed, S.; Panda, S. R.; Kwatra, M.; Sahu, B. D.; Naidu, V. Perillyl Alcohol Attenuates NLRP3 Inflammasome Activation and Rescues Dopaminergic Neurons in Experimental In Vitro and In Vivo Models of Parkinson's Disease. *ACS Chem. Neurosci.* **2022**, *13* (1), 53–68. https://doi.org/10.1021/acschemneuro.1c00550.

(18) Hao, Y.; Huang, J.; Ma, Y.; Chen, W.; Fan, Q.; Sun, X.; Shao, M.; Cai, H. Asiatic Acid Inhibits Proliferation, Migration and Induces Apoptosis by Regulating Pdcd4 via the PI3K/Akt/MTOR/P70S6K Signaling Pathway in Human Colon Carcinoma Cells. *Oncol. Lett.* **2018**, *15* (6), 8223–8230. https://doi.org/10.3892/ol.2018.8417.

(19) Kumar, A.; Rajappan, R.; Kini, S. G.; Rathi, E.; Dharmarajan, S.; Sreedhara Ranganath Pai, K. E-Pharmacophore Model-Guided Design of Potential DprE1 Inhibitors: Synthesis, in Vitro Antitubercular Assay and Molecular Modelling Studies. *Chem. Pap.* **2021**, *75* (10), 5571–5585. https://doi.org/10.1007/s11696-021-01743-3.

(20) Oda, A.; Saijo, K.; Ishioka, C.; Narita, K.; Katoh, T.; Watanabe, Y.; Fukuyoshi, S.; Takahashi, O. Predicting the Structures of Complexes between Phosphoinositide 3-Kinase (PI3K) and Romidepsin-Related Compounds for the Drug Design of PI3K/Histone Deacetylase Dual Inhibitors Using Computational Docking and the Ligand-Based Drug Design Approach. *J. Mol. Graph. Model.* **2014**, *54*, 46–53. https://doi.org/10.1016/J.JMGM.2014.08.007.

(21) Feng, T. T.; Zhang, Y. J.; Chen, H.; Fan, S.; Han, J. G. The Binding Mechanism of a Novel Nicotinamide Isostere Inhibiting with TNKSs: A Molecular Dynamic Simulation and Binding Free Energy Calculation. *J. Biomol. Struct. Dyn.* **2016**, *34* (3), 517–528. https://doi.org/10.1080/07391102.2015.1043580.

(22) Ash, J.; Fourches, D. Characterizing the Chemical Space of ERK2 Kinase Inhibitors Using Descriptors Computed from Molecular Dynamics Trajectories. *J. Chem. Inf. Model.* **2017**, *57* (6), 1286–1299. https://doi.org/10.1021/acs.jcim.7b00048.

(23) Kumar, A.; Rathi, E.; Kini, S. G. E-Pharmacophore Modelling, Virtual Screening, Molecular Dynamics Simulations and in-Silico ADME Analysis for Identification of Potential E6 Inhibitors against Cervical Cancer. *J. Mol. Struct.* **2019**, *1189*, 299–306. https://doi.org/10.1016/j.molstruc.2019.04.023.

(24) Homeyer, N.; Gohlke, H. Free Energy Calculations by the Molecular Mechanics Poisson-

Boltzmann Surface Area Method. *Mol. Inform.* **2012**, *31* (2), 114–122. https://doi.org/10.1002/MINF.201100135.

(25) Wang, E.; Sun, H.; Wang, J.; Wang, Z.; Liu, H.; Zhang, J. Z. H.; Hou, T. End-Point Binding Free Energy Calculation with MM/PBSA and MM/GBSA: Strategies and Applications in Drug Design. *Chem. Rev.* **2019**, *119* (16), 9478–9508. https://doi.org/10.1021/ACS.CHEMREV.9B00055.

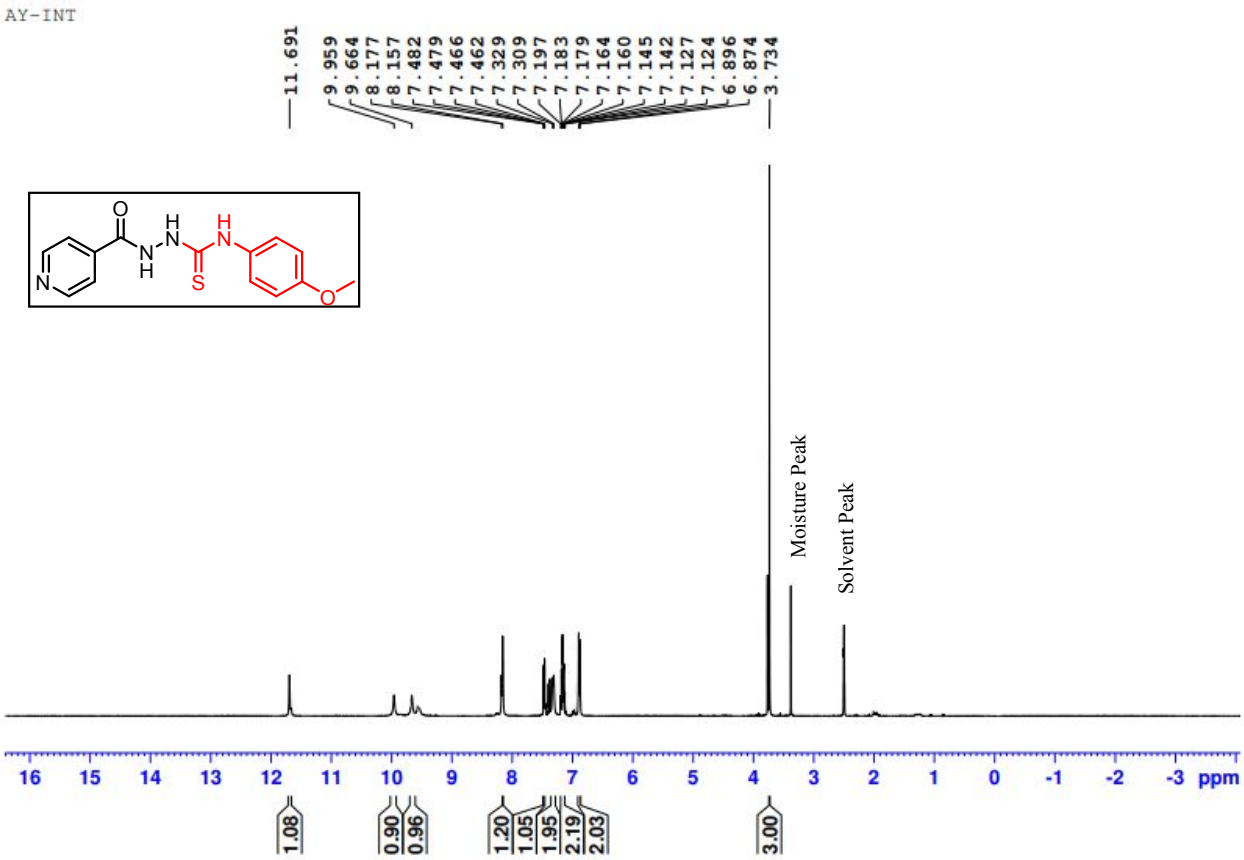

Figure S4. ^{1}H NMR spectra of compound 11a (AY-INT) DMSO d6 (500 MHz).

^{1}H NMR spectra of DMSO-D6 the moisture peaks comes at 3.35 ppm and solvent peaks comes at 2.5 ppm. ^{13}C NMR spectra of DMSO-D6 peaks appears at 39.7 ppm.

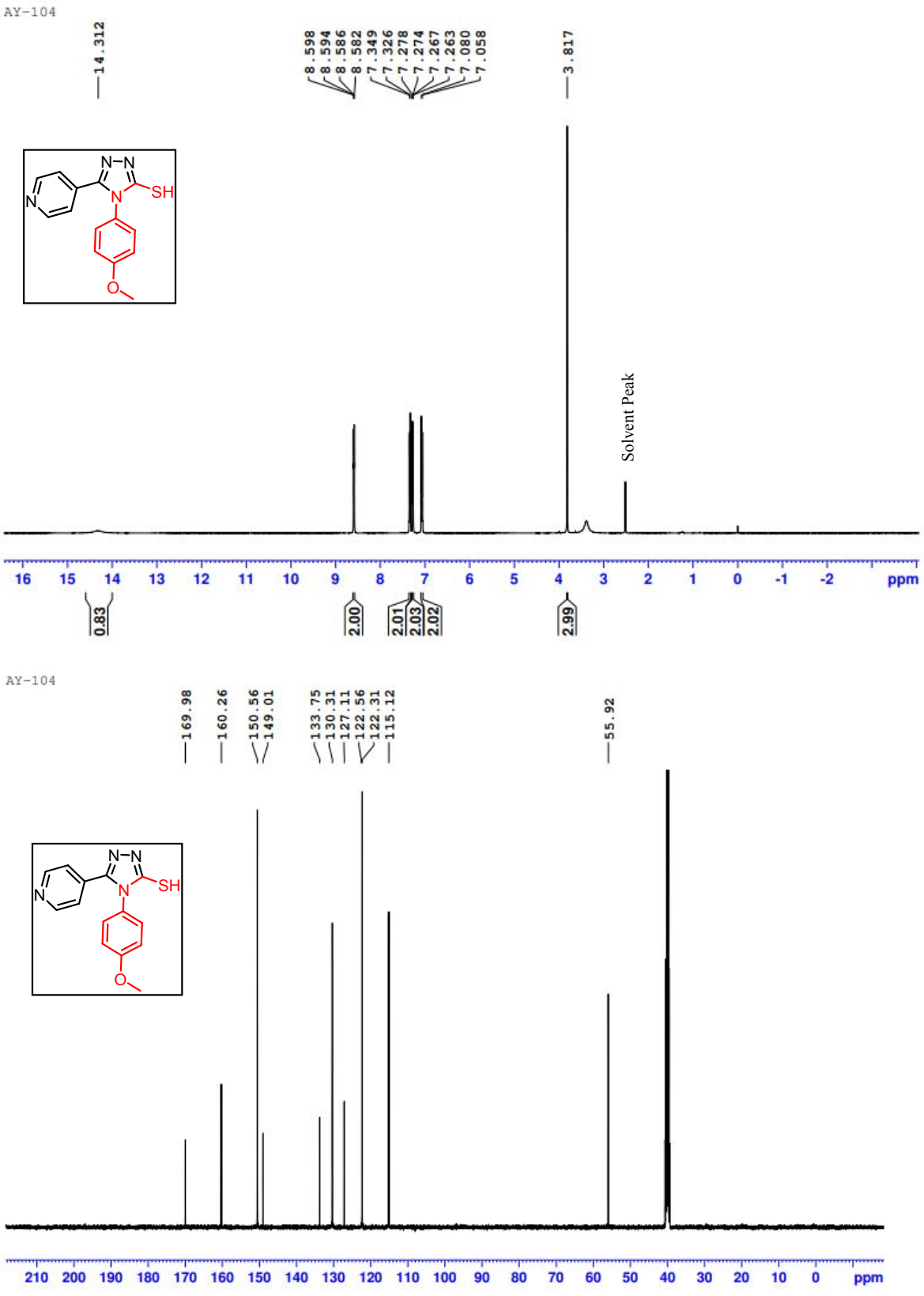

Figure S5. ^{1}H and ^{13}C NMR spectra of compound **12a** (AY-104) DMSO d6 (500 MHz).

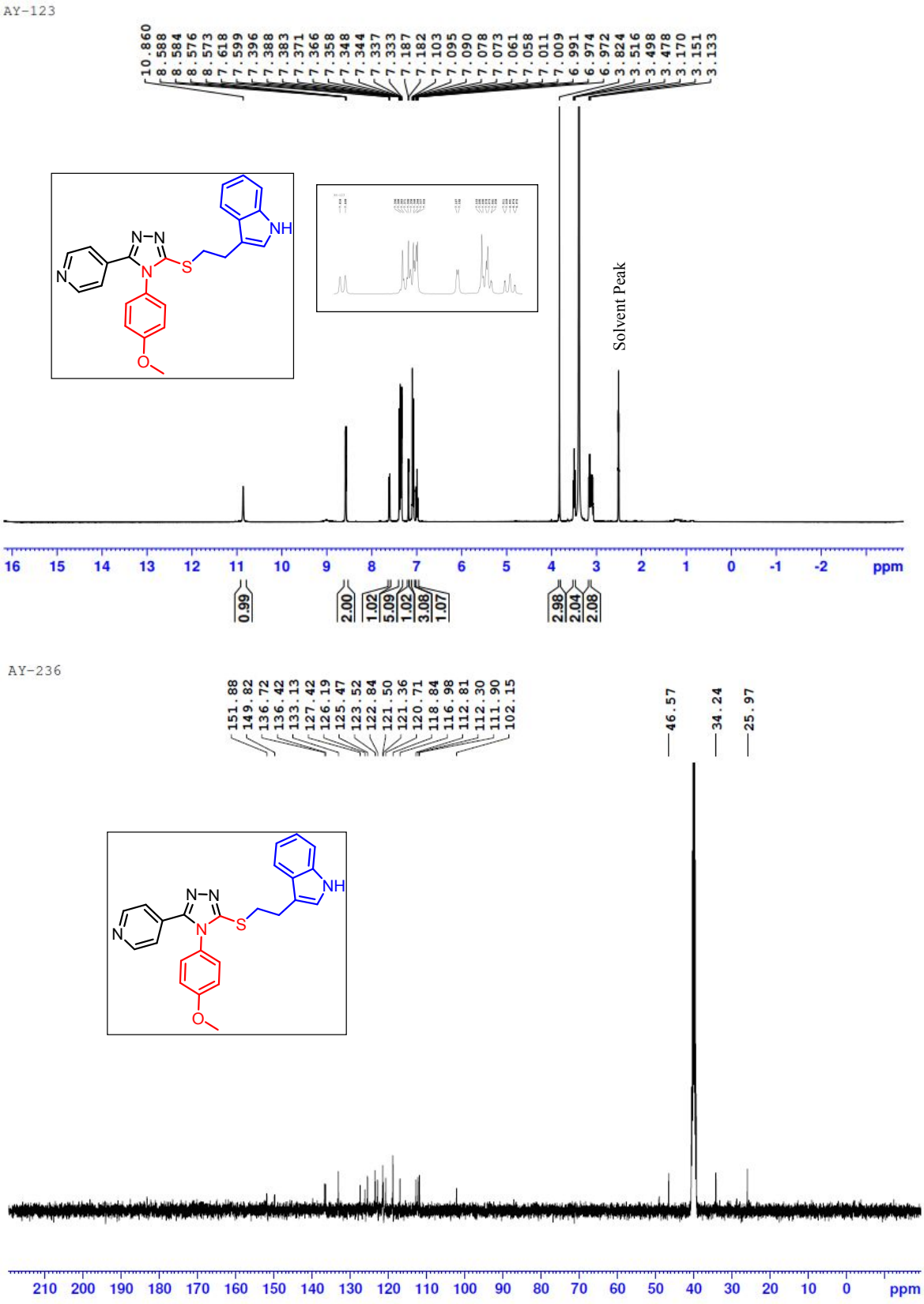

Figure S6. ^{1}H and ^{13}C NMR spectra of compound **14a** (AY-236) DMSO d6 (400 MHz).

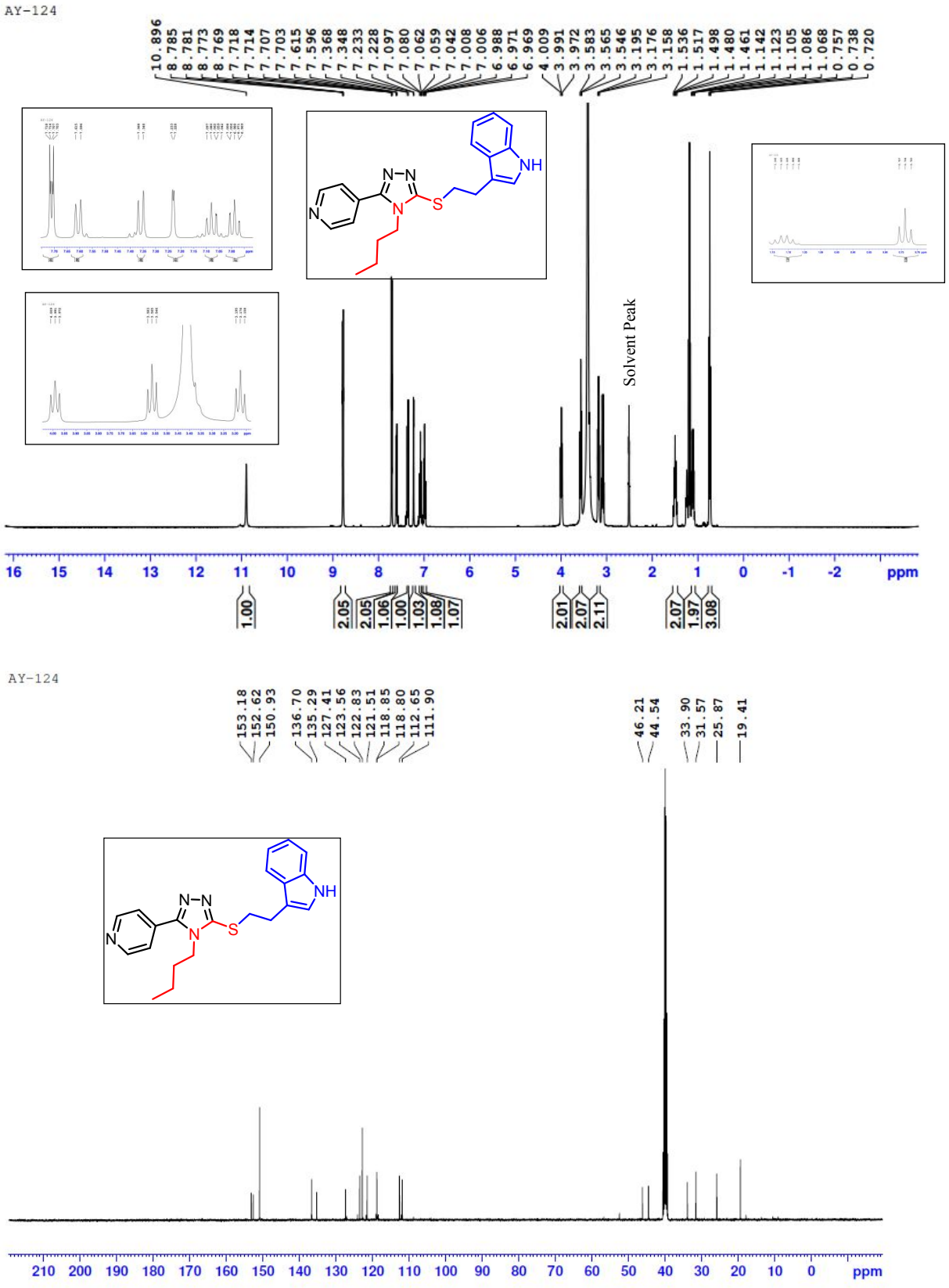

Figure S7. ^{1}H and ^{13}C NMR spectra of compound **14b** (AY-124) DMSO–d_6 (400 MHz).

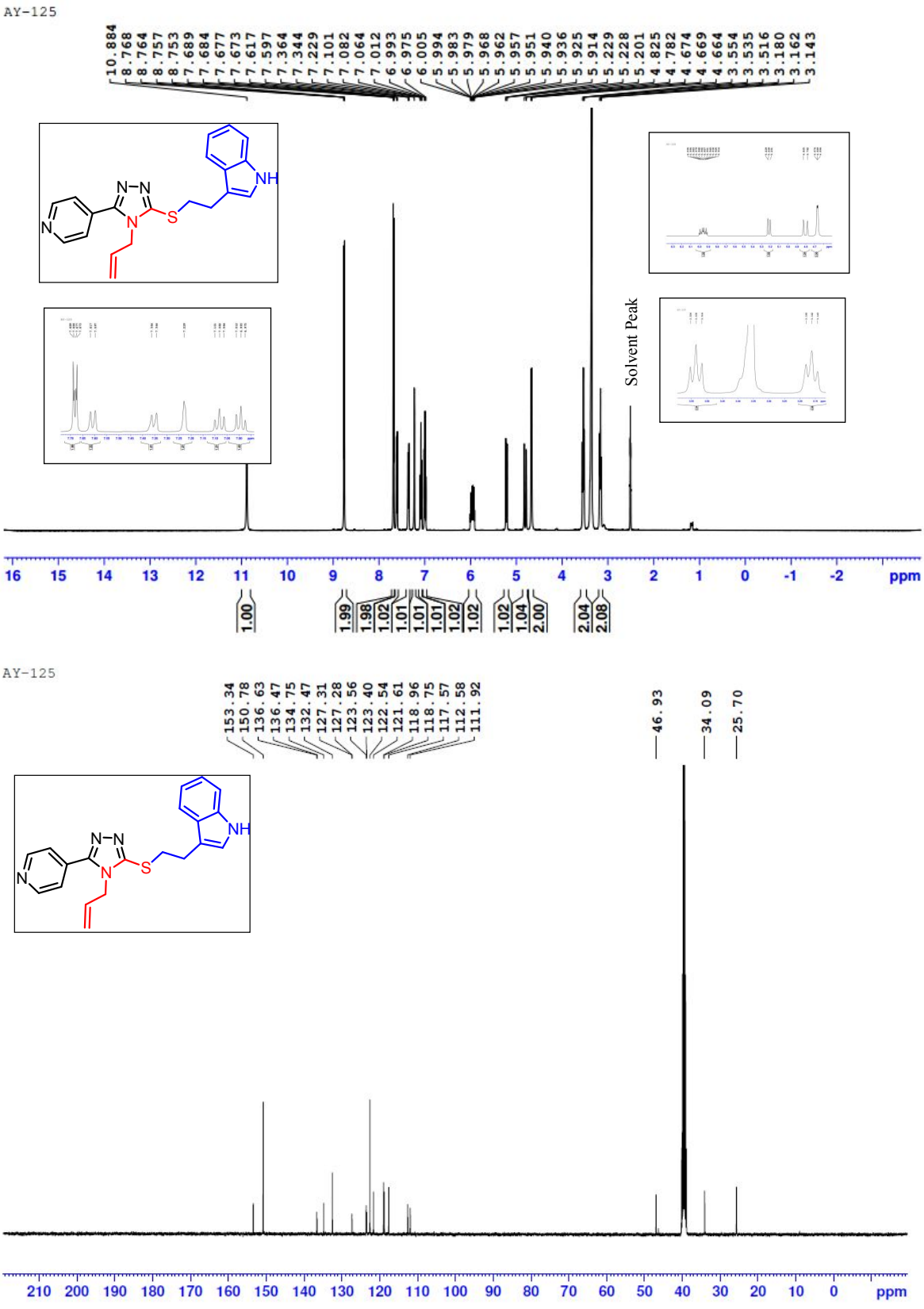

Figure S8. ^{1}H and ^{13}C NMR spectra of compound **14c** (AY-125) DMSO–d_6 (400 MHz).

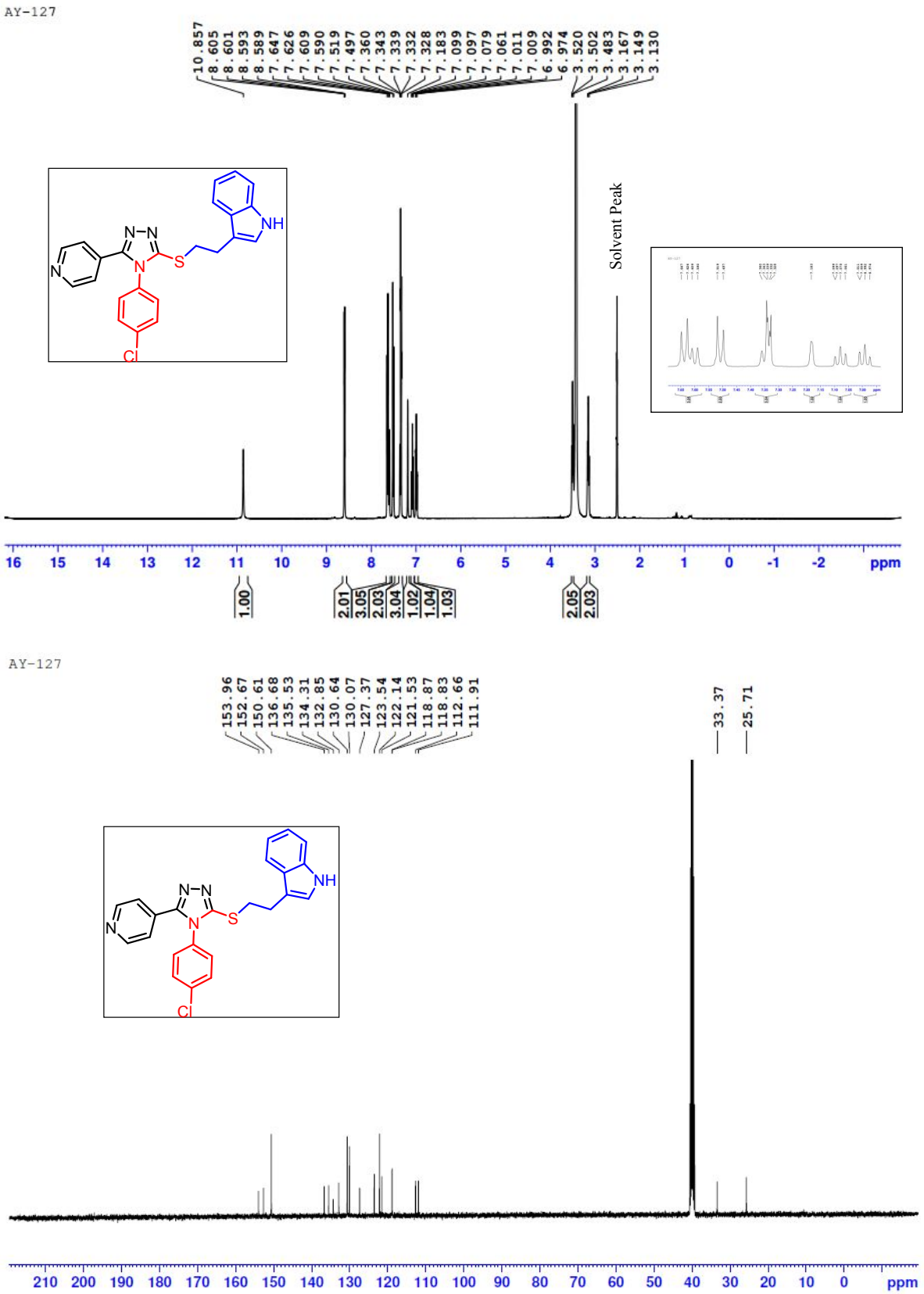

Figure S9. ^{1}H and ^{13}C NMR spectra of compound **14d** (AY-127) DMSO–d_6 (400 MHz).

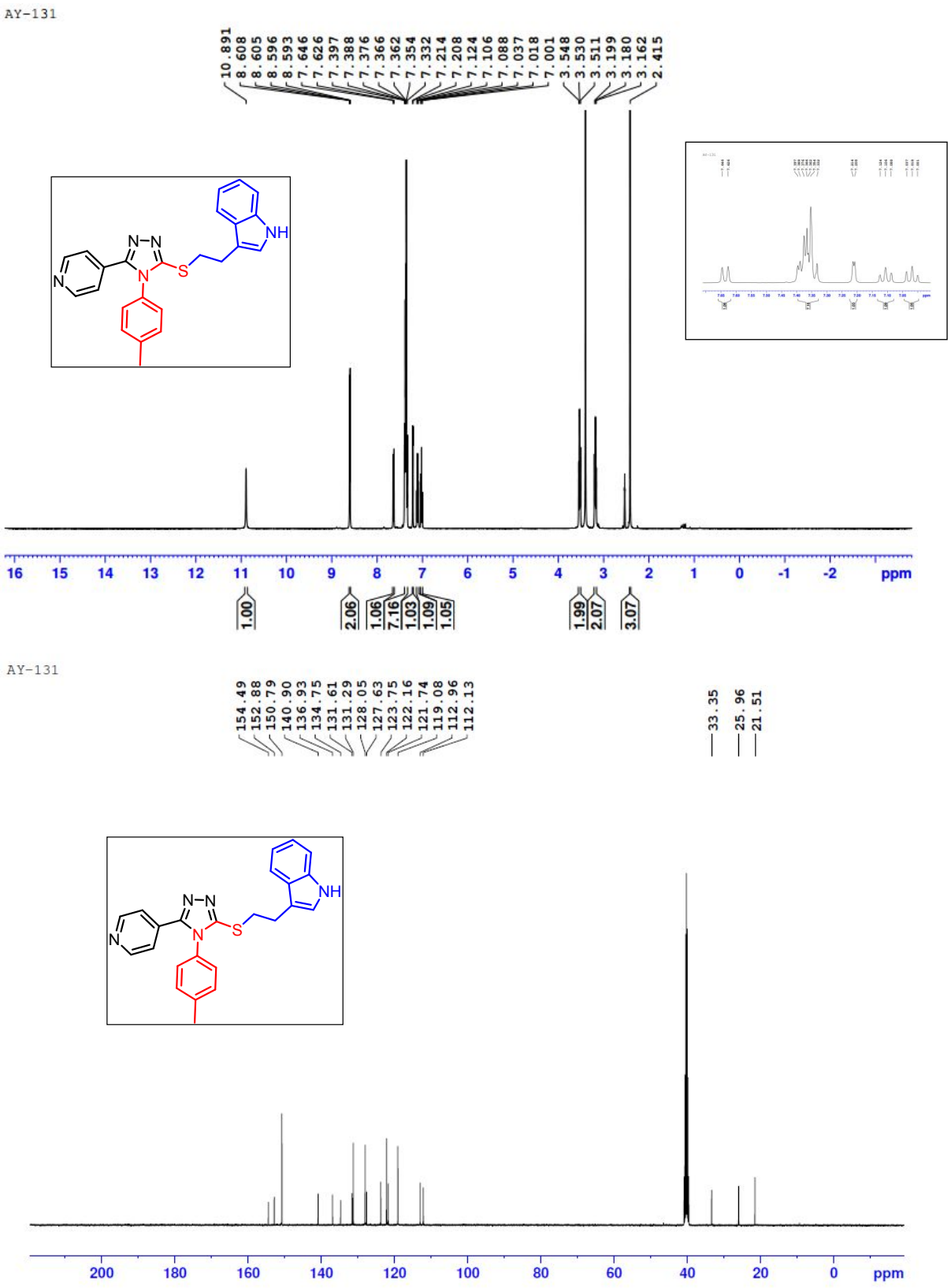

Figure S10. ^{1}H and ^{13}C NMR spectra of compound **14e** (AY-131) DMSO–d_6 (400 MHz).

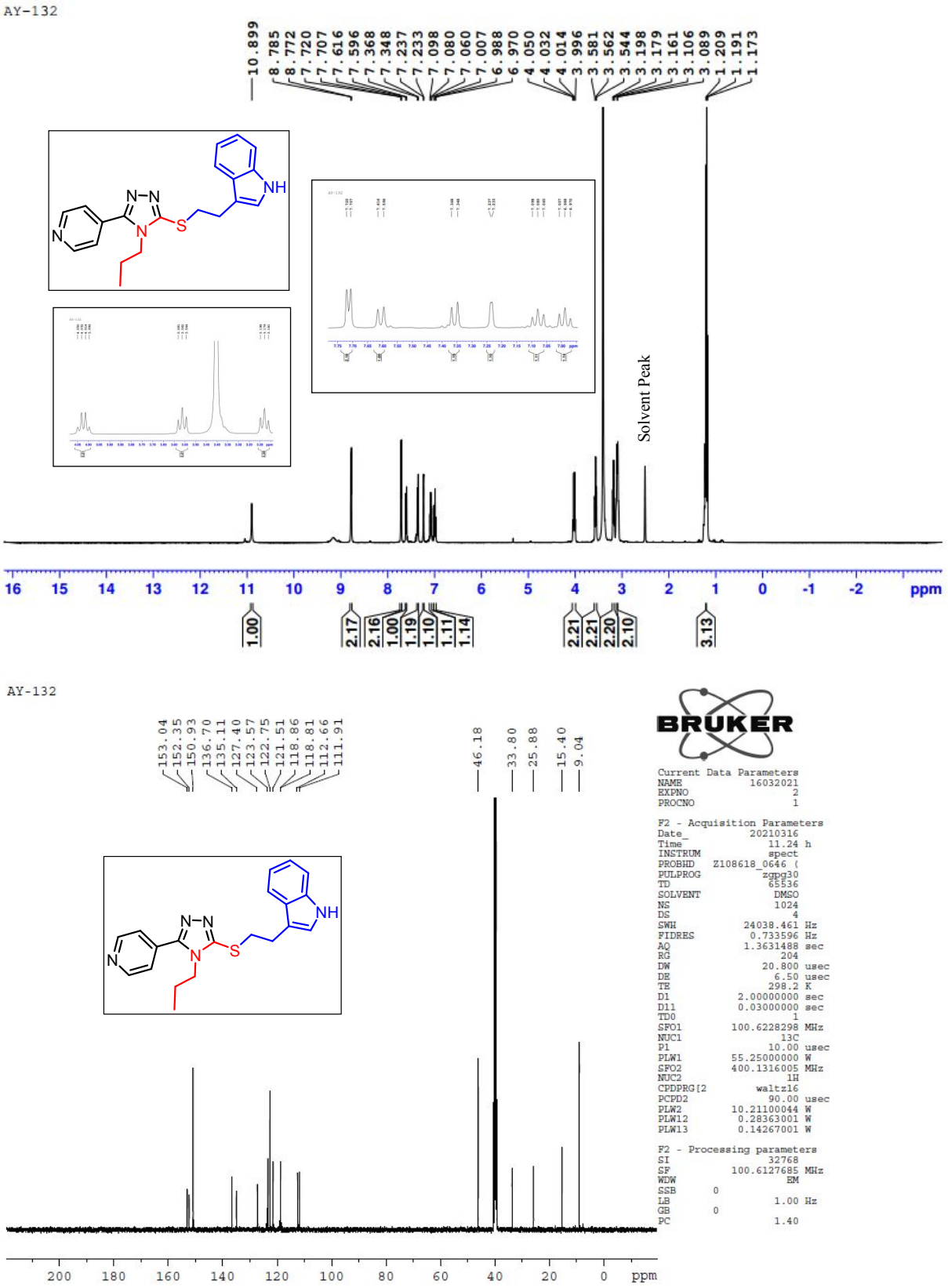

Figure S11. ^{1}H and ^{13}C NMR spectra of compound **14f** (AY-132) DMSO–d_6 (400 MHz).

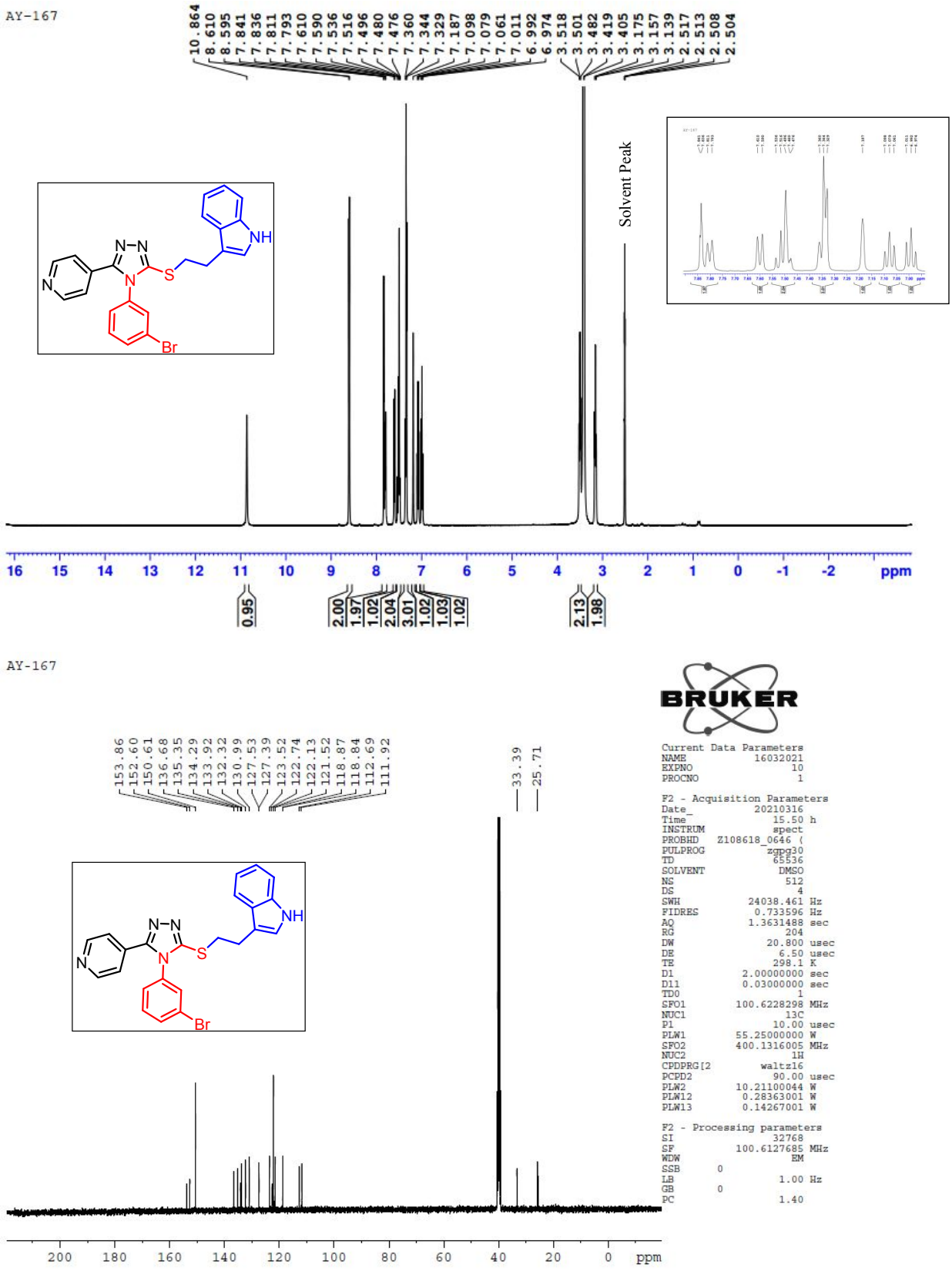

Figure S12. ^{1}H and ^{13}C NMR spectra of compound **14g** (AY-167) DMSO–d_6 (400 MHz).

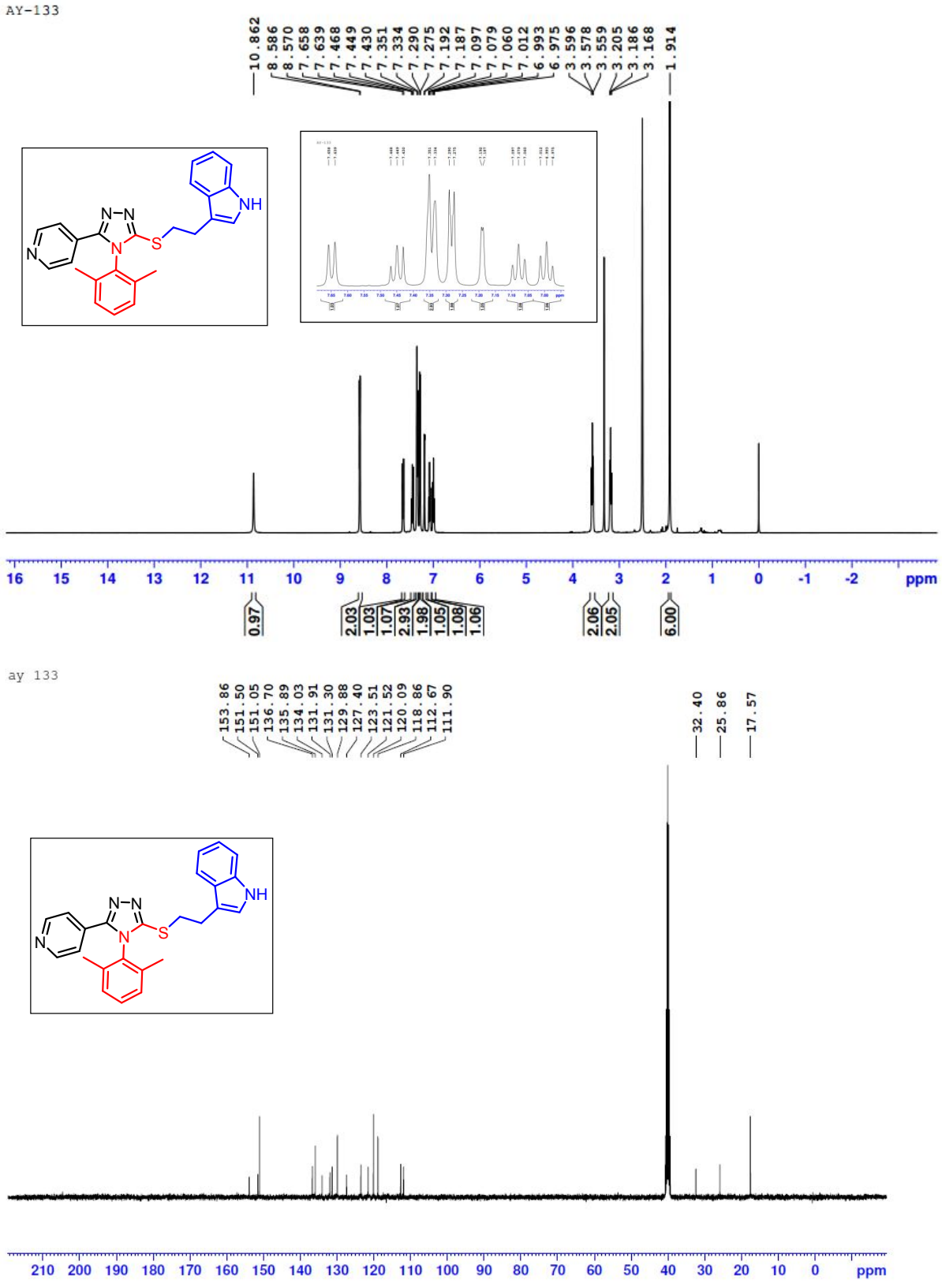

Figure S13. ^{1}H and ^{13}C NMR spectra of compound **14h** (AY-133) DMSO–d_6 (400 MHz).

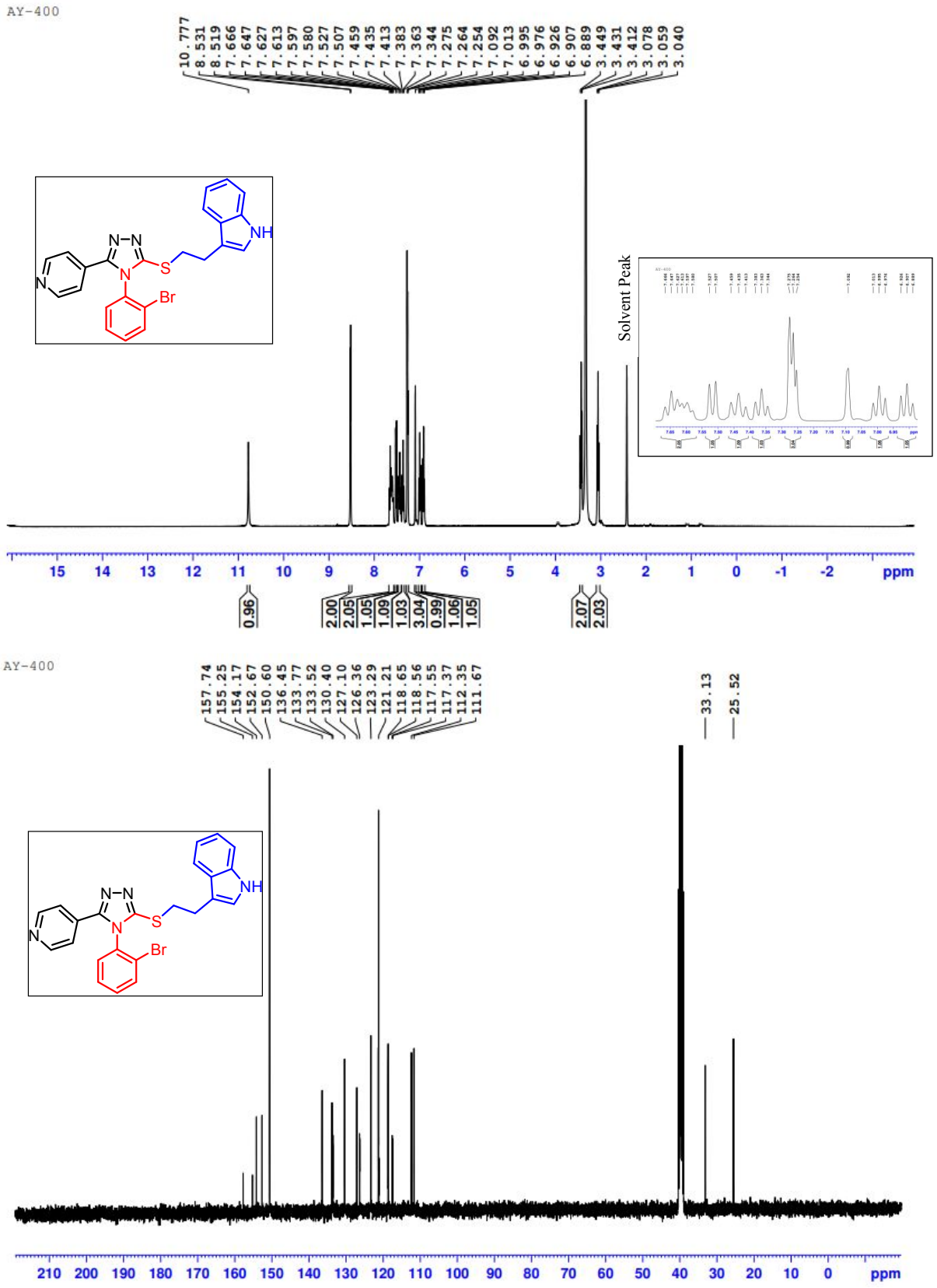

Figure S14. ^{1}H and ^{13}C NMR spectra of compound **14i** (AY-400) DMSO–d_6 (400 MHz).

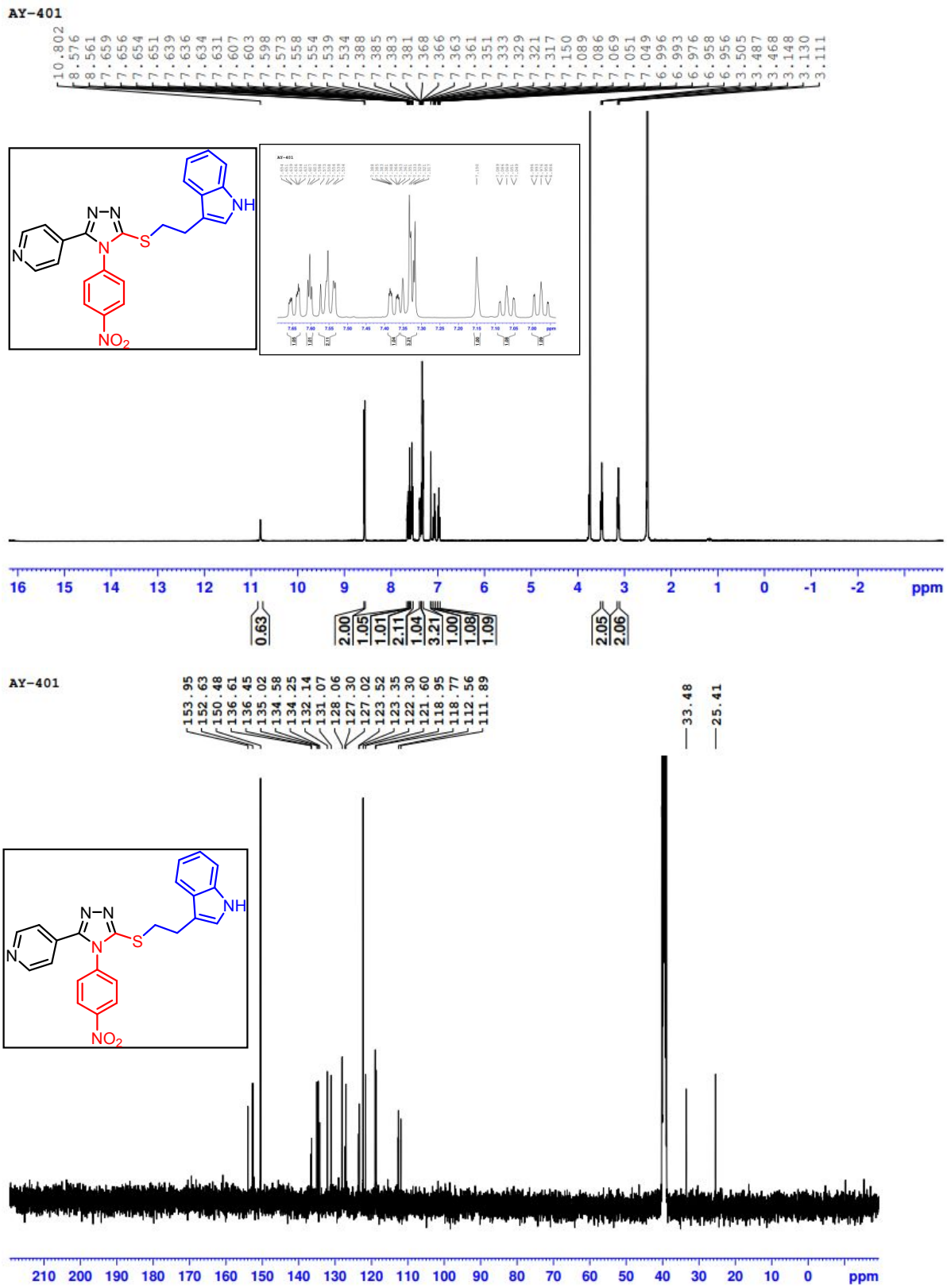

Figure S15. ^{1}H and ^{13}C NMR spectra of compound **14j** (AY-401) DMSO–d_6 (400 MHz).

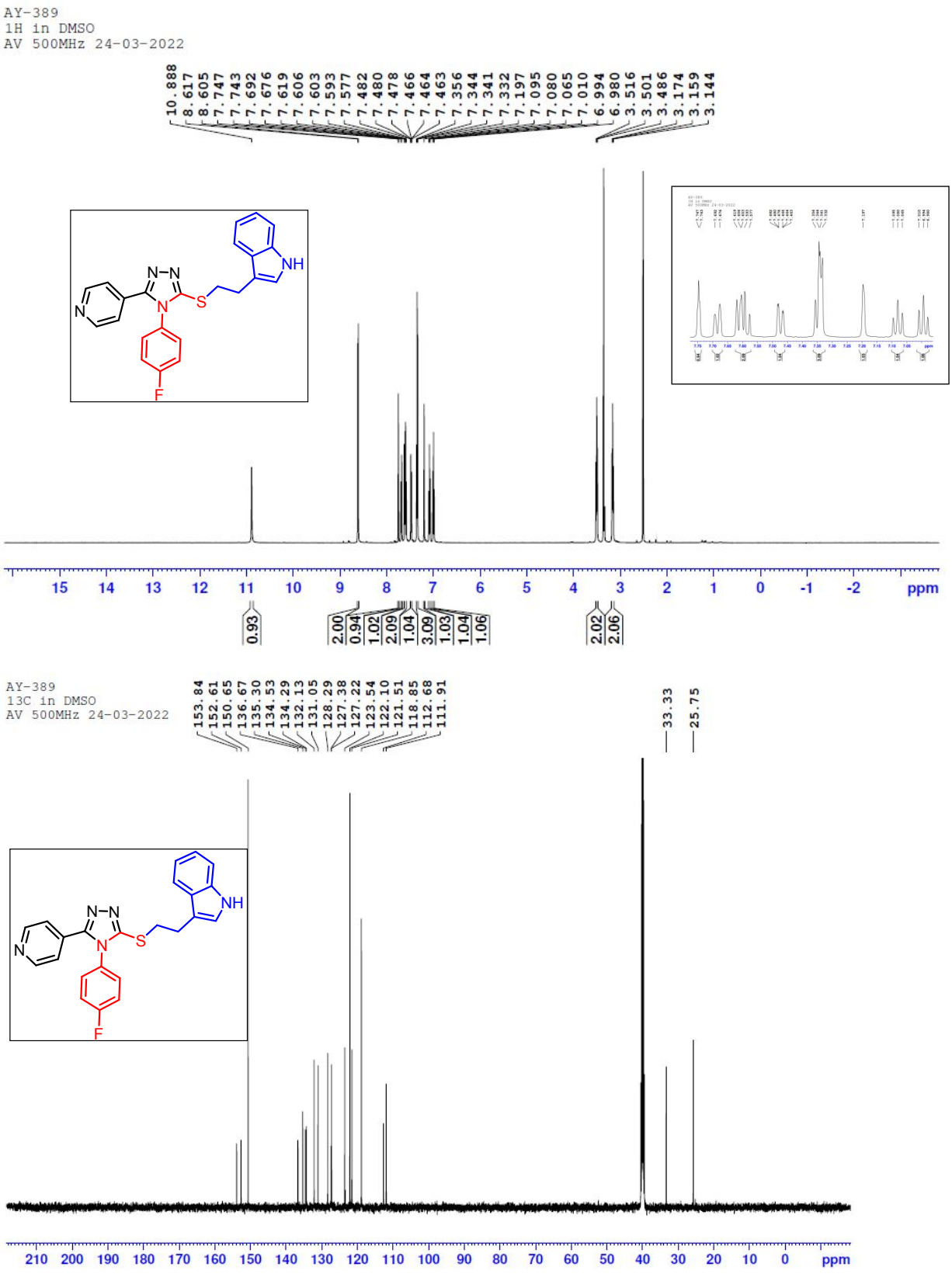

Figure S16. ^{1}H and ^{13}C NMR spectra of compound **14k** (AY-389) DMSO–d_6 (500 MHz).

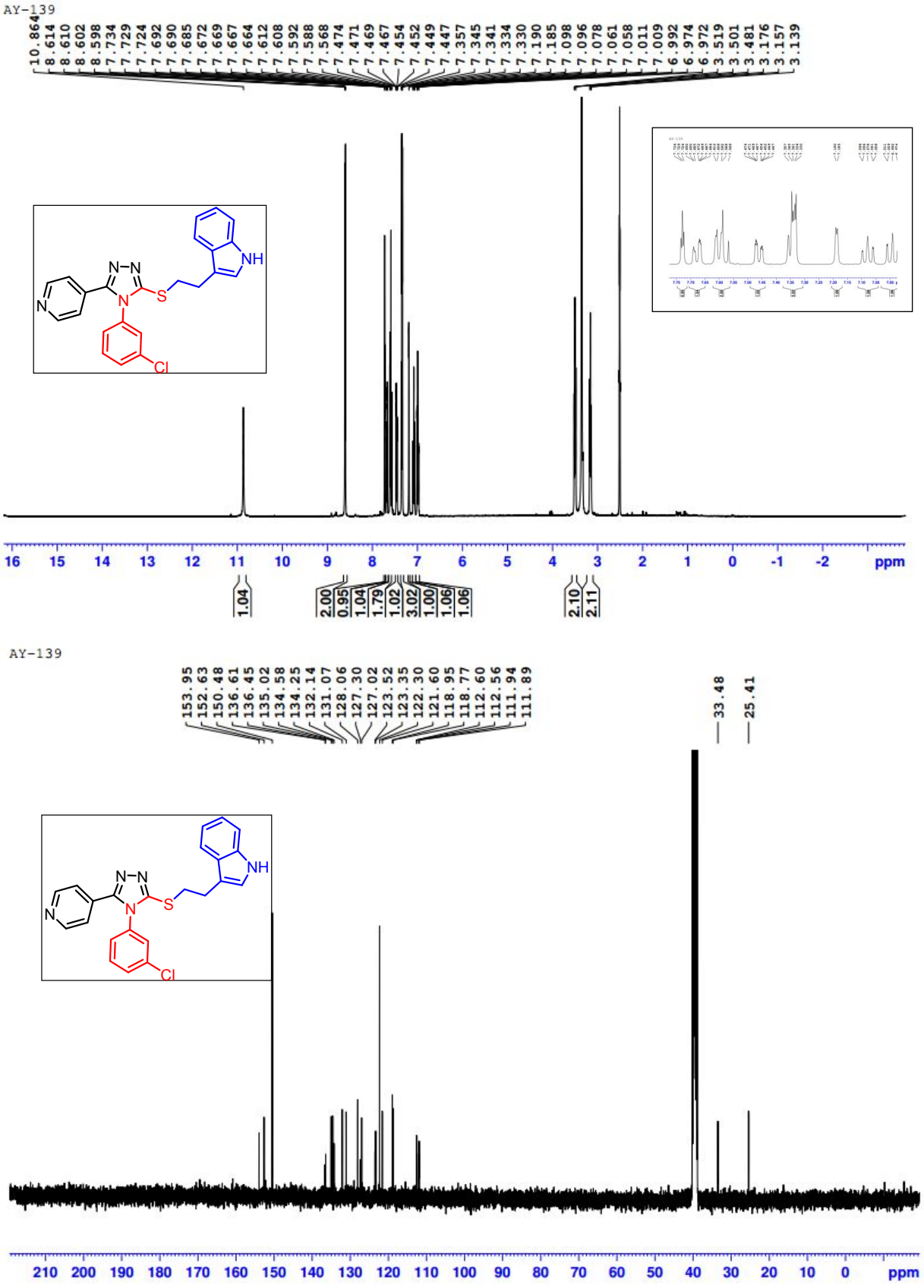

Figure S17. ^{1}H and ^{13}C NMR spectra of compound **14l** (AY-139) DMSO–d_6 (400 MHz).

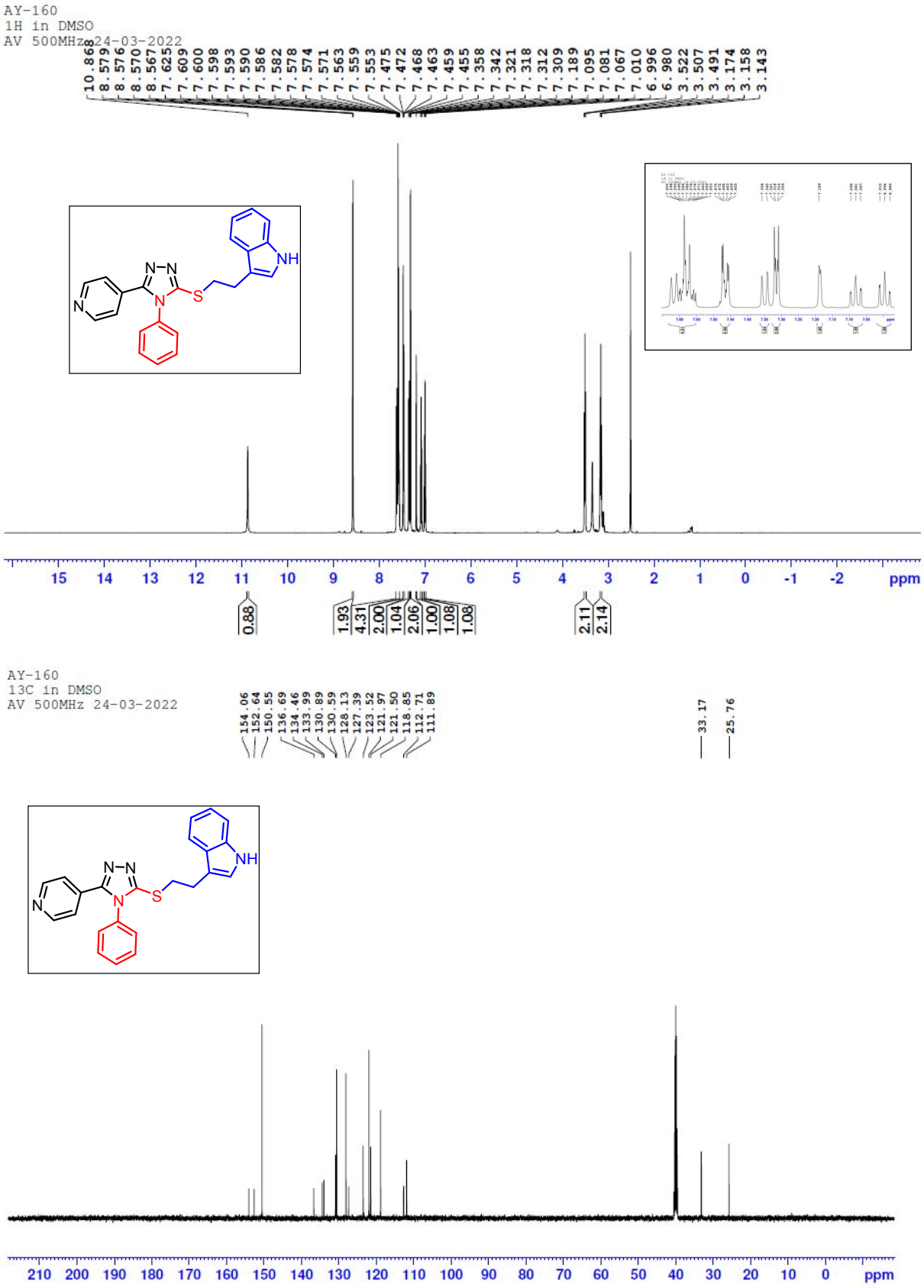

Figure S18. ^{1}H and ^{13}C NMR spectra of compound **14m** (AY-160) DMSO–d_6 (500 MHz).

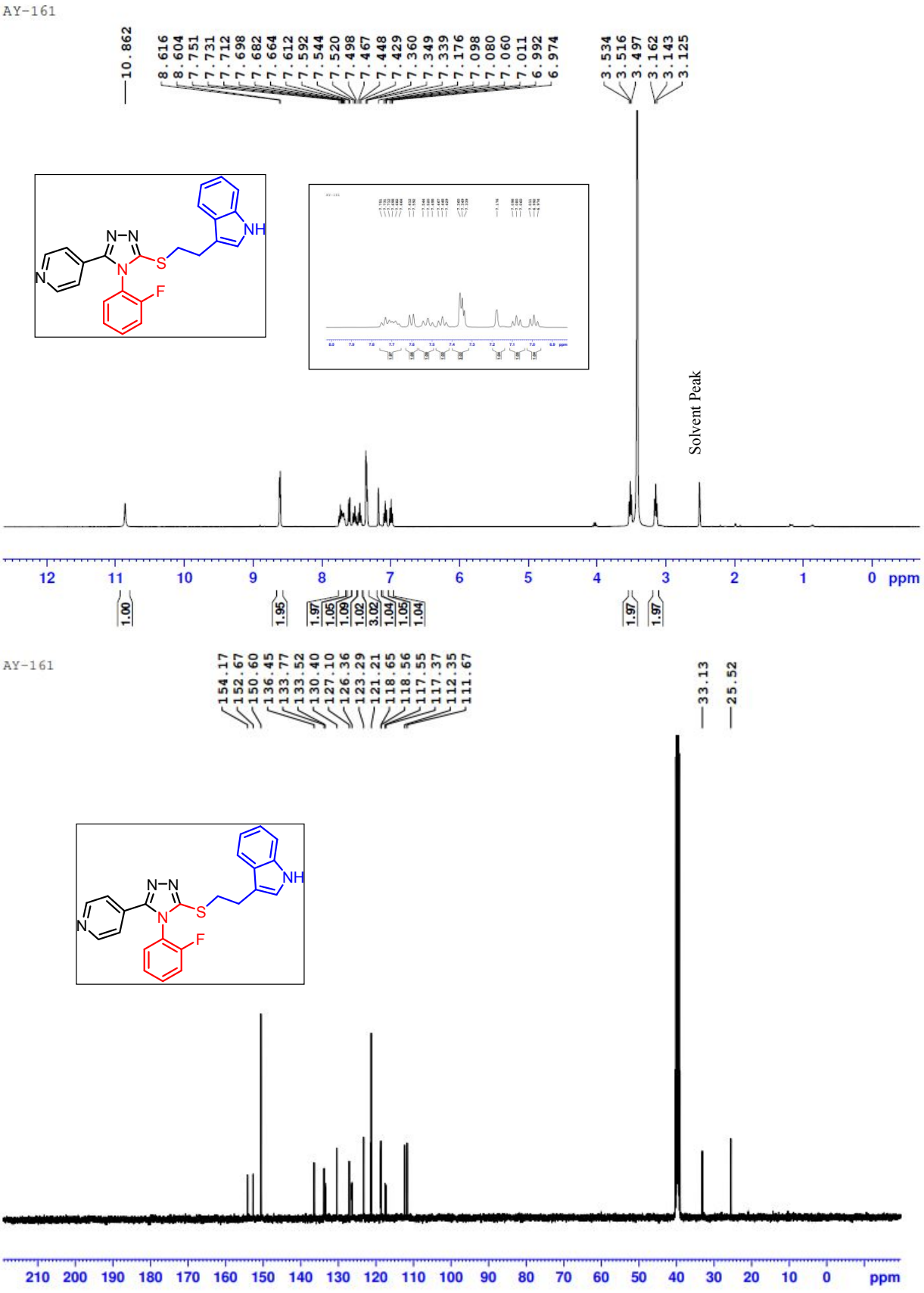

Figure S19. ^{1}H and ^{13}C NMR spectra of compound **14n** (AY-161) DMSO–d_6 (400 MHz).

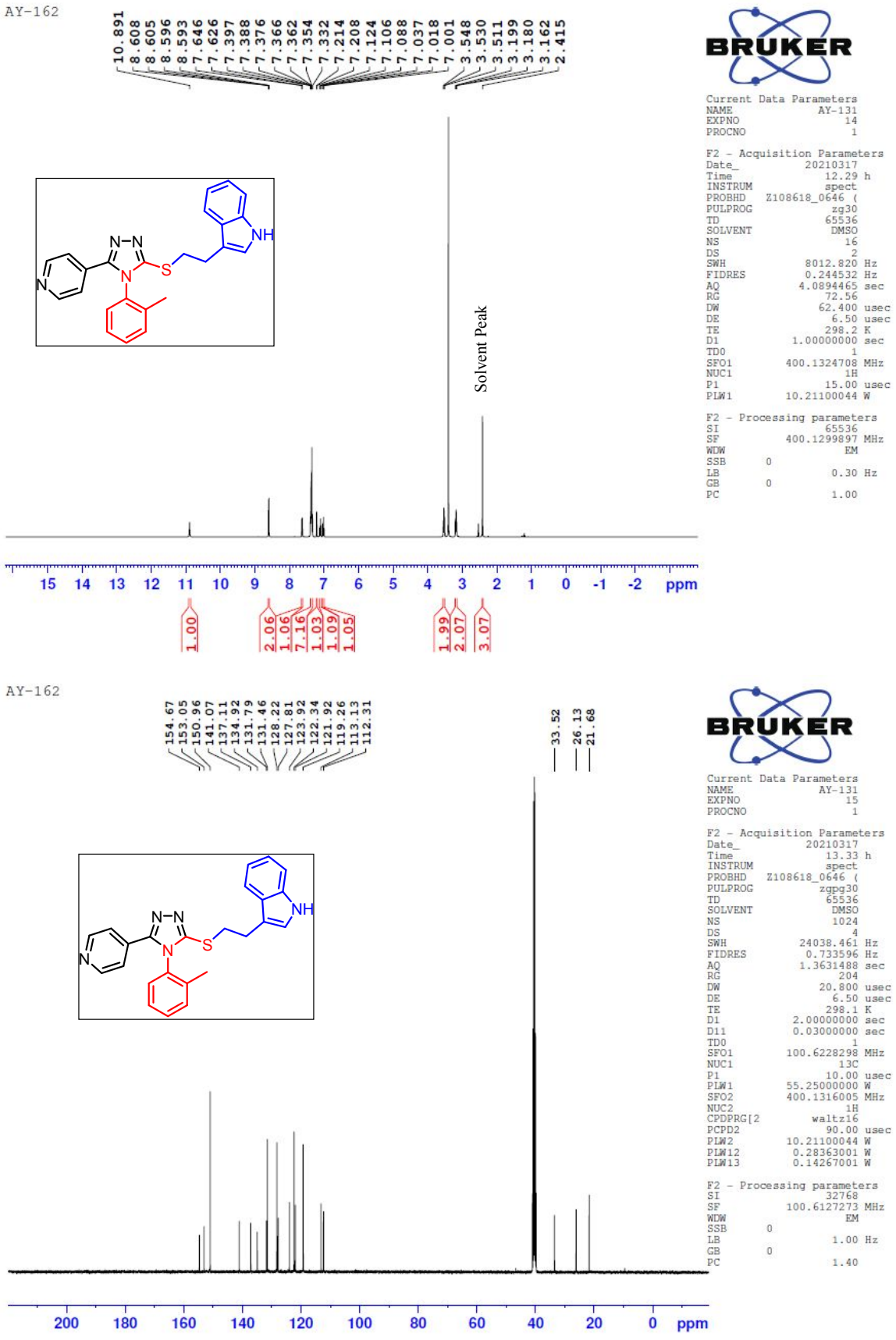

Figure S20. ^{1}H and ^{13}C NMR spectra of compound **14o** (AY-162) DMSO–d_6 (400 MHz).

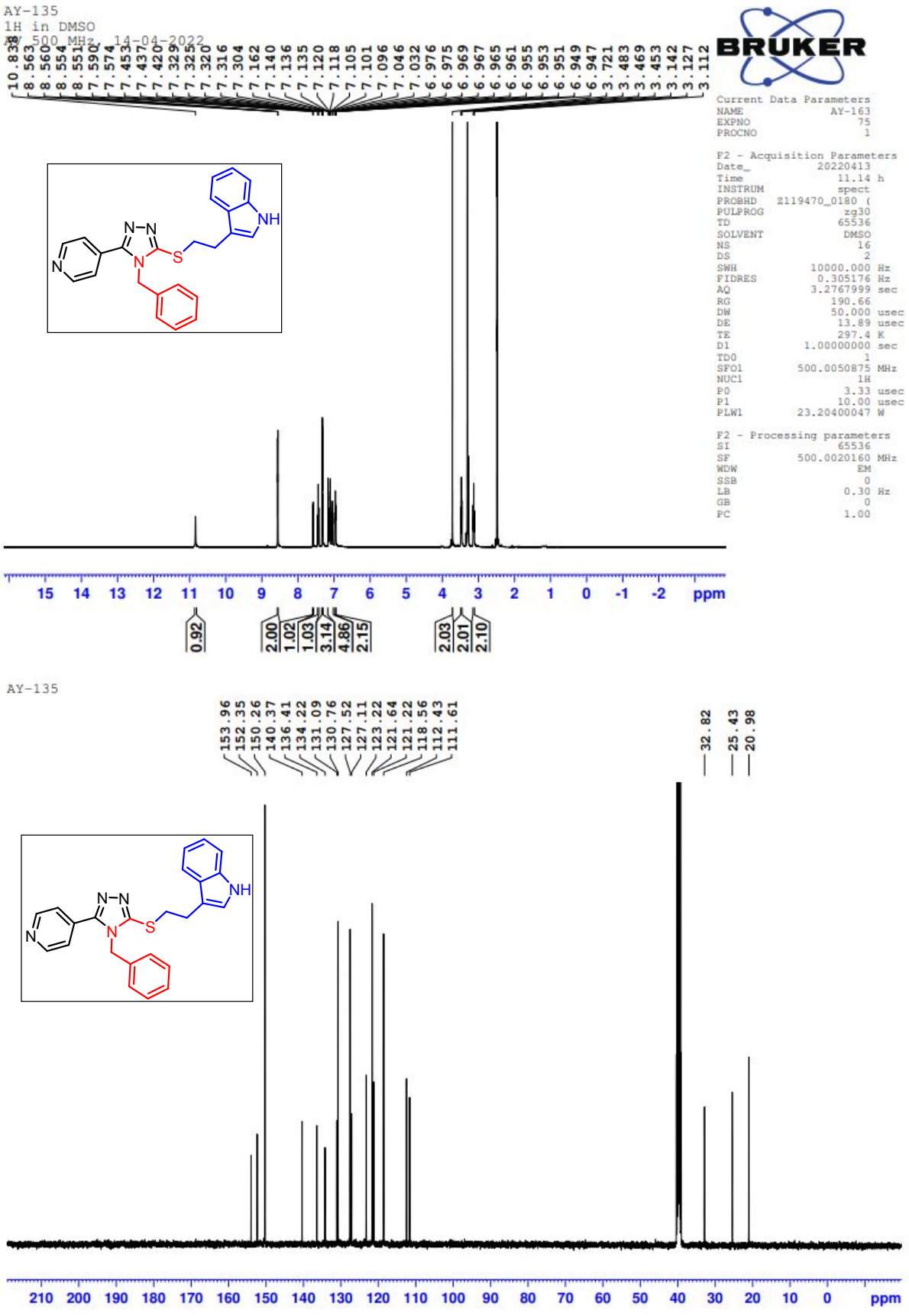

Figure S21. ^{1}H and ^{13}C NMR spectra of compound **14p** (AY-135) DMSO–d_6 (400 MHz).

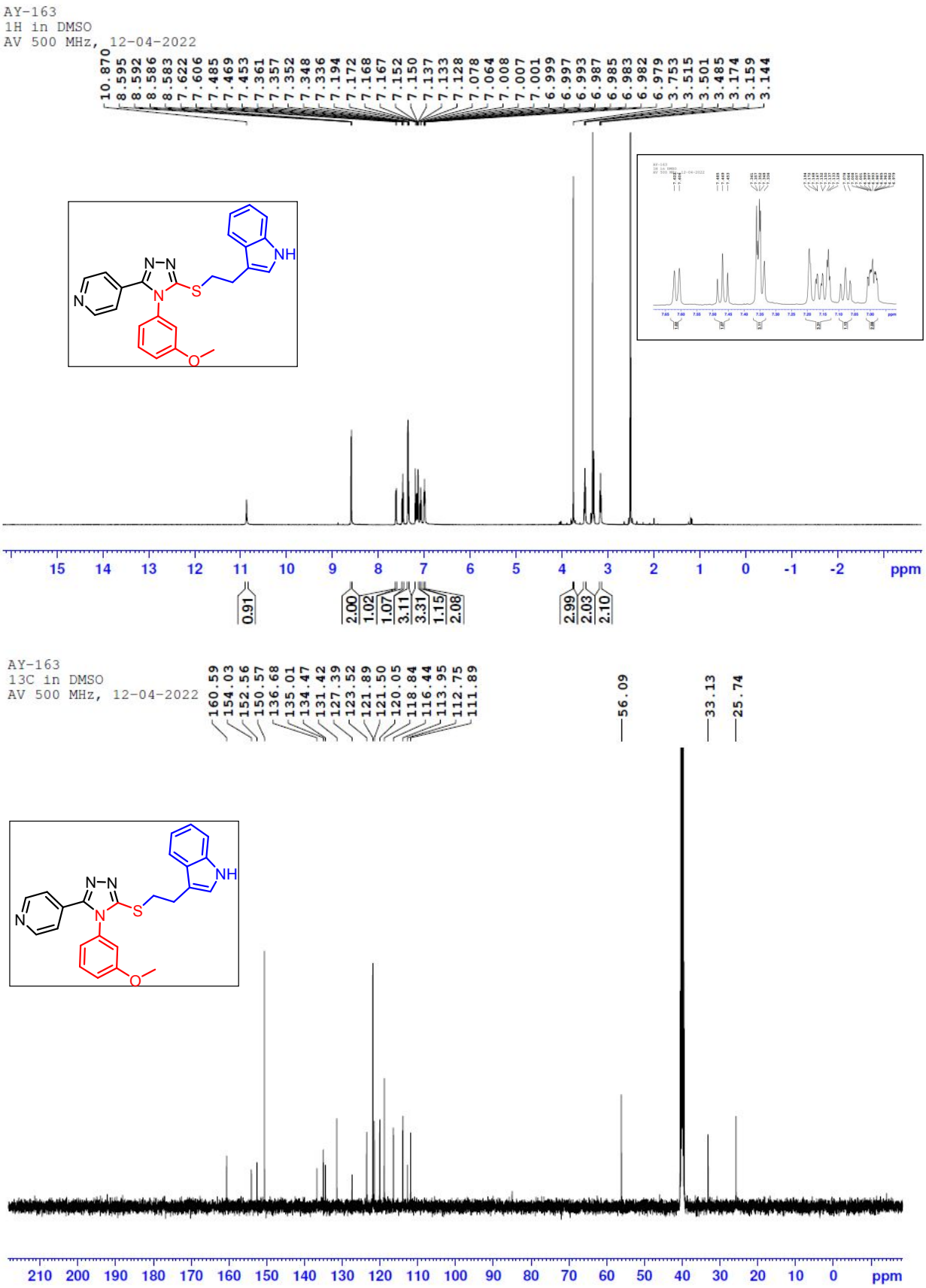

Figure S22. ^{1}H and ^{13}C NMR spectra of compound **14q** (AY-136) DMSO–d_6 (500 MHz).

HPLC Method condition

Name of the samples: 14a, 14n and 14q

Sample preparation: The compound is dissolved in the mixture of acetonitrile and H_2O (1:1) with the help of sonication.

Mobile Phase:

A) 0.1% Formic acid: dissolve 1 ml of formic acid into 1000ml distilled water.
B) Acetonitrile

Chromatographic condition:

Column: Xbridge C18, 5µ 4.6 mm x 250 mm
Column temp: 25 °C
Sample temp: 10 °C
Flow rate: 1 ml/min
Injection volume: 10 µL
Wavelength: 254 nm

Gradient Program:

Time	%B
0.1	10
3	10
7	40
12	90
15	90
16	40
20	10

COMPOUND 14a---98.3 %

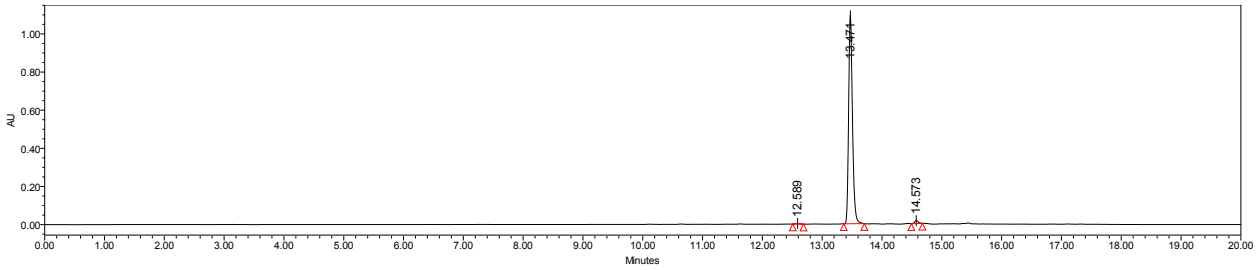

	Name	Retention Time	Area	% Area
1		12.589	17335	0.35
2	A	13.471	4836427	98.30
3		14.573	66124	1.34

COMPOUND 14n---95.72

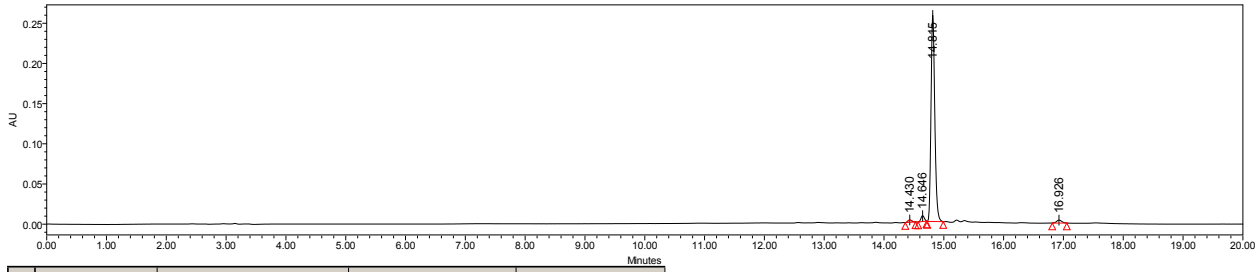

	Name	Retention Time	Area	% Area
1		14.430	13036	1.09
2		14.646	28208	1.36
3	B	14.815	1129997	95.72
4		16.926	21708	1.82

COMPOUND 14q----96.08%

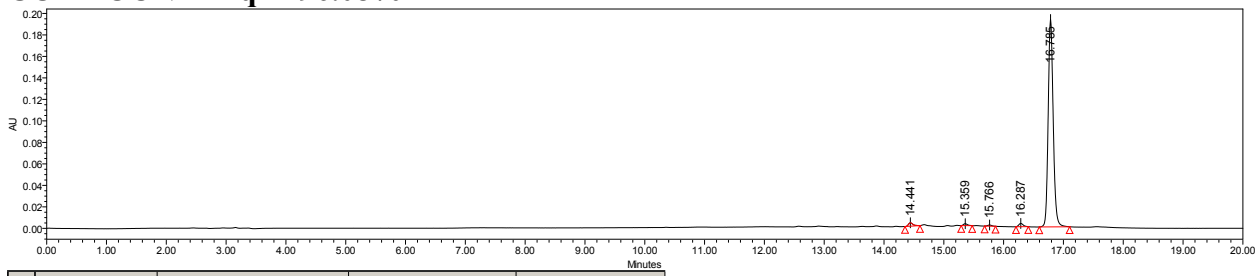

	Name	Retention Time	Area	% Area
1		14.441	16655	1.42
2		15.359	8427	0.72
3		15.766	5046	0.43
4		16.287	15687	1.34
5	C	16.785	1124074	96.08